Russian Chemical Reviews 65 (6) 521 – 536 (1996)

UDC 678.01;537.6

The nature and dynamics of nonlinear excitations in conducting polymers. Heteroaromatic polymers

V A Krinichnyi

Contents

Abstract. The results of studies on the structural, conformational, and dynamic properties of organic conducting polymers by 2 mm EPR spectroscopy are treated systematically and surveyed. The structural and dynamic features of the paramagnetic centres as well as the mechanism of charge transfer in the conducting polymers are discussed. The bibliography includes 73 references.

I. Introduction

Various organic conducting compounds are known at the present time: charge-transfer complexes and radical-ion salts, platinum complexes with cyanide ligands, phthalocyanines, dyes, metal-filled polymers, etc.[1–4] These compounds are of interest from the standpoint of a study of the fundamental principles of charge transfer. Among them, one should distinguish particularly organic conducting polymers such as polyparaphenylene (PPP), polythiophene (PT), polypyrrole (PP), the emeraldine base (EB) and emeraldine salt (ES) form of polyaniline (PANI), polytetrathiafulvalene (PTTF), polyacetylene (PA), etc., which may prove promising in molecular electronics (the spin charge carriers stabilised in the polymers are shown below).[5–7]

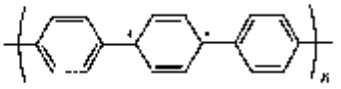

PPP

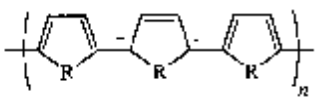

PT (R = S)
PP (R = NH)

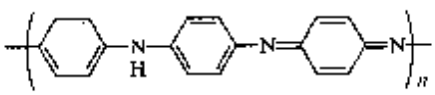

PANI EB

V I **Krinichnyi**. Laboratory for Electrically Conducting Compounds. Institute of Chemical Physics in Chernogolovka, Russian Academy of Sciences, 142432 Chernogolovka, Moscow Region, Russian Federation. Fax (7-096) 515 35 88. Tel. (7-096) 524 50 35

Received 6 July 1995
Uspekhi Khimii 65 (6) 564 – 580 (1996); translated by A K Grzybowski

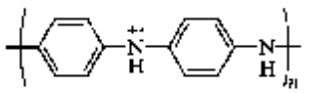

PANI ES

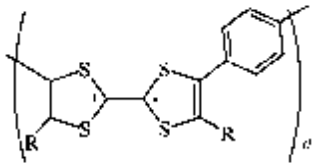

PTTF-1 (R = Et)

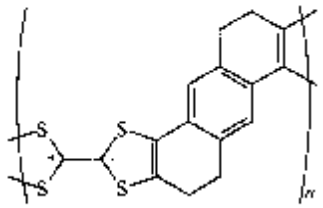

PTTF-2

These compounds are characterised by an anisotropic quasi-one-dimensional (1D) π-conjugated structure and, in contrast to classical polymers, exhibit an electrical conductivity which varies by more than 10 orders of magnitude when the polymer is doped with various counterions.[5] The introduction of BF_4^-, ClO_4^-, AsF_5^-, I_3^-, $FeCl_4^-$, MnO_4^-, etc. anions induces a positive charge on its chains, i.e. leads to a *p*-type conductivity, whereas *n*-type conductivity is achieved by doping the polymer with various alkali metals, for example Li^+, K^+, and Na^+.

The electrodynamic properties of conducting polymers are significantly influenced by their structure, conformation, and the packing of their chains. The globular structure of the polymers is made up of fibrils with a typical diameter of 100 nm, the fibrils consisting in their turn of crystallites. The parameters of the corresponding unit cells of such crystallites are listed in Table 1. The dihedral angle θ between the planes of the monomer units in the polymer, for example in PPP, is ~ 23°.[12] The value of this angle is a result of a compromise balance between the conjugation effect, tending to bring the system to a planar conformation, and the steric repulsion of the hydrogen atoms in the *ortho*-positions, which rules out a planar conformation. The electron density transfer integral I between the monomer units is given by $I \sim \cos \theta$,[13] so that the probability of the 1D-charge transfer in the polymer increases with increase in the planarity of the chain.

Table 1. The unit cell parameters of conducting polymers.

Polymer	System	Parameter / nm			Ref.
		a	*b*	*c*	
PPP	Monoclinic	0.779	0.562	0.426	8
	Orthorhombic	0.781	0.553	0.420	8
PT	Hexagonal	0.950	0.620	1.220	9
PP	Monoclinic	–	0.341	0.718	10
PANI	Monoclinic	0.705	0.860	0.950	11

The overlap of the π orbitals of the monomer rings results in the formation of a band structure of the polymer with gap widths of 3.5 eV (PPP), 2.2 eV (PT), 3.0 eV (PP), 4.0 eV (undoped PANI), and 1.5 eV (ES form of PANI).[10,12] The resonance interaction of the energetically nonequivalent benzenoid and quinonoid forms of the monomers is the cause of the nonlinear topological excitation — the formation of a polaron with a spin of $\frac{1}{2}$, delocalised over 4–5 monomer units of the polymer.[5] The energy levels of such a polaron are located in the forbidden band at a distance Δ_1 below the conductivity band and at a distance Δ_2 above the valence band. $\Delta_1 = \Delta_2 = 0.7$ eV for PPP, $\Delta_1 = 0.9$ eV and $\Delta_2 = 0.45$ eV for PP, and $\Delta_1 = 0.7-0.9$ eV and $\Delta_2 = 0.5-0.6$ eV for the other conducting polymers.[14] For sufficiently high levels of doping, pairs of polarons may recombine with formation of longer spin-less bipolarons.

Conducting polymers contain paramagnetic centres (PC) at a concentration $N = 10^{16}-10^{21}$ spins g^{-1},[15,16] so that one of the most promising methods for their investigation is EPR spectroscopy, which makes it possible to obtain varied and unique information about the structure of the polymer and about the nature and properties of the paramagnetic centres (their concentration, mobility, relaxation, etc.). Such studies are as a rule carried out at relatively low recording frequencies ($\nu_e \leqslant 10$ GHz). In these bands, conducting polymers, like other π-electron systems, usually give rise to a single symmetrical line with a width between the peaks $\Delta B_{pp} = 0.02-1.70$ mT and a g-factor close to that for a free electron ($g_e = 2.00232$).[15,16] The deviation from g_e can occur on interaction of an unpaired electron with heteroatoms or the alkali metals of the dopants.[17,18] For a sufficiently high level of doping, the so called Dyson line,[15,19] leading to the asymmetry of the spectrum, is manifested as a consequence of the increase in the electrical conductivity of the sample. However, in the study of conducting polymers with $\nu_e \leqslant 10$ GHz, investigators have encountered fundamental difficulties associated mainly with the low spectral resolution and a strong spin–spin exchange in this EPR frequency range.

It was shown previously in relation to various organic radicals[20–23] that the information content and the accuracy of the method increase significantly on passing to the 2 mm band for the recording of the EPR spectra. In this range, it is possible to achieve the separate detection of paramagnetic centres with similar magnetic parameters, which permits a more accurate determination of the components of their anisotropic g-factor and also makes it possible to investigate the anisotropic dynamics of the radicals and of their microenvironment. The method makes it possible to study in fair detail different properties of *cis*- and *trans*-polyacetylenes as well as the relaxation and dynamic features of nonlinear charge carriers (solitons) in *trans*-polyacetylene.[24]

The present review is devoted to the consideration of the principal results of the study at the 2 mm EPR band of the structural and conformational properties of certain other conducting polymers as well as the charge carriers present in them, the dynamics of which is described by the universal nonlinear Korteweg-de Vries equations of motion.

II. Polyparaphenylene

The concentration of unpaired electrons in PPP depends significantly on the polymerisation methods and may vary within the range $10^{17}-10^{19}$ spins g^{-1}.[15,16] The line width increases on doping and such broadening may depend both on the degree of doping and on the atomic number of the alkali metal of the dopant. The latter finding indicates an appreciable spin–orbital interaction between the dopant molecule and the unpaired electron. As in other conducting polymers, the charge transfer is effected mainly by polarons in lightly doped PPP and by bipolarons in a quasi-metallic sample.[8,12,14]

Various PPP samples (in the form of films), synthesised by the electrochemical oxidation of benzene in a $C_5H_5C_5H_4NCl-AlCl_3$ melt, have been investigated by the EPR method: the initial evacuated PPP sample doped with Cl^{3-} anions (PPP-1); the same sample after storage over four days (PPP-2); the initial sample brought into contact with atmospheric oxygen for several seconds (PPP-3); the initial dedoped sample (PPP-4); the sample redoped with BF_4 anions (PPP-5).[25]

In measurements at the 3 cm EPR band, the PPP-1, PPP-2, and PPP-3 samples give rise to a single asymmetric line with a distinct Dyson form and $g = 2.0029$ (Fig. 1*a*). The line asymmetry factor A/B (the ratio of the amplitudes of the positive and negative peaks) varies as a function of the conductivity of the sample. When the Cl_3^- dopant is removed, i.e. on passing from the PPP-1 to the PPP-4 sample, the above spectrum is transformed into an axially symmetrical spectrum with $g_\perp = 2.0034$ and $g_\parallel = 2.0020$ (Fig. 1*b*). This is accompanied by the broadening of the spectral lines and also by a sharp decrease in the concentrations of spins and charge carriers (Table 2). It is noteworthy that neither in the case of PPP nor in the case of other π-conjugated polymers, investigated previously at the 3 cm EPR band, were axially symmetrical spectra recorded.[15] The above form of the spectrum remains unchanged on further doping of the neutral PP with BF_4 anions (PPP-5), but in this case some decrease in the spin concentration and a change in the sign of its temperature dependence are observed (Table 2). The minimum excitation energy of the unpaired electron $\Delta E_{\pi\pi^*} = 5.2$ eV, close to the energy of the first ionisation potential of polycyclic aromatic hydrocarbons,[13]

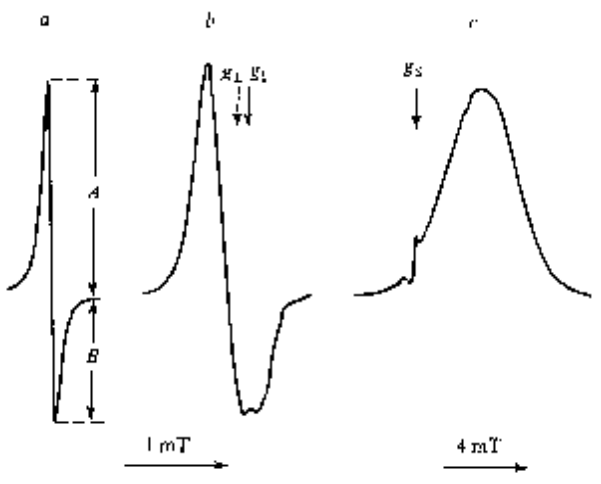

Figure 1. Typical 3 cm EPR absorption spectra of PPP-1 PPP-3 (*a*) and PPP-4 and PPP-5 (*b*) samples and the 2 mm in-phase dispersion spectrum of the PPP-4 and PPP-5 samples (*c*) recorded at room temperature. The narrow line on the right-hand spectrum belongs to the $(DBTTF)_2PtBr_6$ reference standard with $g_s = 2.00411$. The measured magnetic parameters are presented.

Table 2. The concentration of the paramagnetic centres (N), the d.c. (σ_{dc}) and a.c. (σ_{ac}) conductivities ($\nu_0 = 140$ GHz), the line asymmetry parameter (A/B), the line width (ΔB_{pp}), and the spin–lattice relaxation time (τ_1) for polyparaphenylene samples at $T = 300$ K.

Parameters	Sample				
	PPP-1	PPP-2	PPP-3	PPP-4	PPP-5
$10^{-17} N$/spin g^{-1}	120	320	210	4	0.6
σ_{dc}/S m^{-1}	$10^3 - 10^4$	—	—	10^{-6}	1
$10^{-5} \sigma_{ac}$/S m^{-1}	3	4	1.4	—	—
A/B	2.3	2.5	1.4	—	—
ΔB_{pp}/mT	0.09	0.12	0.22	0.37[a]	0.47[a]
$10^6 \tau_1$/s	0.4	0.5	0.2	~100	~100

[a] The width of the high-field spectral component is presented.

may be calculated, using the difference $\Delta g = g_\perp - g_\parallel = 1.4 \times 10^{-3}$, from the equation

$$\Delta E_{\sigma\pi^*} = \frac{2\lambda_C \rho_C}{\Delta g}, \tag{1}$$

where λ_C is the constant for the spin–orbital interaction of the unpaired electron with a carbon nucleus and ρ_C the electron density on carbon.[26] Thus the paramagnetic centres in PPP-4 and PPP-5 can be localised in the vicinity of the polycyclic hydrocarbon cross-links, as predicted previously.[15]

At the 2 mm EPR band, the PPP-4 and PPP-5 samples give rise to a bell-shaped signal (Fig. 1*c*), which arises as a result of the manifestation of the effect due to the rapid adiabatic passage of a nonuniformly broadened line.[27] The spin–lattice relaxation time of the paramagnetic centres in these samples, estimated from their spectra, is $\tau_1 \approx 10^{-4}$ s. The rapid passage effects will be examined in greater detail below.

The rate of the spin–spin exchange of the paramagnetic centres in the neutral and redoped PPP has been determined as $\nu_{ex} = 4 \times 10^7$ s^{-1} by analysing the form of the 3 cm and 2 mm EPR spectra.[25] For PPP-1, this quantity is 1.8×10^8 s^{-1} owing to the greater concentration and mobility of the paramagnetic centres. The isotropic g-factor ($\langle g \rangle = \frac{1}{3}(g_\parallel + 2g_\perp)$ for a neutral sample is close to the g-factor for the polymer doped with Cl_3^- anions. This finding indicates the averaging of the components of the g-tensor for the paramagnetic centres as a consequence of the spin 1D-diffusion along the polymer chain of the PPP-1 sample at a minimal rate:

$$\nu_{1D}^0 \geq \frac{(g_\perp - g_\parallel)\mu_B B_0}{h}, \tag{2}$$

where μ_B is the Bohr magneton, B_0 the magnetic field strength, and h the Planck constant. For the PPP sample doped with Cl_3^- anions, this quantity is $\nu_{1D}^0 \geq 6.8 \times 10^6$ s^{-1}. Indeed the effective rate of the spin 1D-diffusion, calculated from the equation

$$(\Delta B_{pp}^{noh})^3 = \frac{\gamma_e (\Delta B_\perp^{loc})^4}{\nu_{1D}}, \tag{3}$$

(here ΔB_{pp}^{noh} is the width of the line between the peaks of the PPP-1 samples, $\Delta B_\perp^{loc}$ the width of the perpendicular component of the spectrum of the PPP-4 and PPP-5 samples, and γ_e the gyromagnetic ratio for the electron) proved to be $\nu_{1D} \approx 9 \times 10^{10}$ s^{-1} at room temperature. The temperature dependence of the electrical conductivity of the PPP-1 sample, determined using alternating current from the function $A/B(T)$, has the form $\sigma_{ac}(T) \sim T^{-1/2}$. This shows that several conduction mechanisms, including the interchain variable range hopping (VRH) charge transfer and isoenergetic tunnelling of the charge carriers, operate in the doped PPP. The sharp decrease in spin concentration and in the rates of the spin exchange and relaxation processes on dedoping of the sample (transition from PPP-1 to PPP-4) indicates the annihilation of the majority of the polarons, the 1D-diffusion of which determines the effective electronic relaxation of the entire spin system.

Thus the data obtained make it possible to conclude that, in the highly doped PPP-1 sample, the charge is transferred mainly by the mobile polarons, whereas in PPP-5 charge transfer is effected by diamagnetic bipolarons. On electrochemical substitution of the Cl_3^- anion by the BF_4^- anion, the location of the latter may differ from that of the dopant in the initial sample. The morphology of the PPP redoped with BF_4^- anions may be close to that in the neutral film (PPP-4).

It has been established[25] that a film of PPP synthesised from the $C_5H_7C_5H_4NCl-AlCl_3$ melt is characterised by a decrease in the number of benzenoid monomers and an increase in that of the quinonoid ones. This leads to a more ordered structure and to a planar conformation of the polymer, which apparently prevents the collapse of the spin charge carriers to a bipolaron in the highly doped polymer. On dedoping, the anions are 'washed out', which results in an increase in the packing density of the polymer chains. This may prevent the intrafibrillar introduction of BF_4^- anions and may lead to localisation of the dopant molecules in the interfibrillar free volume of the polymer matrix. Such a conformational transition apparently alters the mechanism of charge transfer in the course of the redoping of PPP.

III. Polythiophene

The 3 cm EPR spectrum of neutral PT consists of a single symmetrical line with $g \approx 2.0026$ and a width $\Delta B_{pp} = 0.8$ mT[15] which indicates the localisation of the spin on the polymer chain and its weak interaction with the sulfur atoms. The low concentration of paramagnetic centres ($N \approx 7 \times 10^{-5}$ of a spin per monomer unit) is associated with the comparatively low degree of defectiveness of this compound. The EPR signal of lightly doped poly(3-methyl)thiophene represents a superposition of a Gaussian line due to the localised paramagnetic centres with $g_1 = 2.0035$ and $\Delta B_{pp} \approx 0.7$ mT and a Lorentzian line with $g_2 = 2.0029$ and $\Delta B_{pp} = 0.15$ mT. The latter is characteristic of delocalised paramagnetic centres.[28] The overall concentration of paramagnetic centres in this sample is $\sim 3 \times 10^{19}$ spins cm^{-3} or about one spin per 300 thiophene rings. After doping, a single Lorentzian component remains. It is symmetrical up to a doping level $z \leq 0.25$ (z is the number of dopant molecules per polymer monomer unit), but becomes asymmetric (Dyson line) for $z > 0.3$. The appearance of the Dyson-like line is accompanied by a significant decrease in the spin–spin and spin–lattice relaxation times,[29] which may be a consequence of the increase in the dimensionality of the system. Analysis of the variation of the paramagnetic susceptibility $\chi(z)$ showed that the number of paramagnetic polarons increases during the doping process in the polymer, the polarons recombining to diamagnetic bipolarons for high values of z.

Powder-like PT samples,[30] containing different counterions, were investigated at the 2 mm EPR band. The samples were obtained electrochemically from thiophene and bithiophene.

At the 3 cm EPR band, the PT samples synthesised from thiophene and doped with BF_4^-, ClO_4^-, and I_3^- ions give rise to symmetrical lines with $g \approx g_e$ and a width ΔB_{PP}, which varies slightly over a wide temperature range (Table 3), whereas in the spectrum of the PT synthesised from bithiophene and doped with I_3^- anions the lines are appreciably broadened as the temperature increases.

The PT spectra recorded at the 2 mm EPR band are distinguished by a greater variety (Fig. 2). Axially symmetrical spectra, indicating the localisation of the paramagnetic centres on the polymer chains, are characteristic of the polymers $PT(BF_4^-)$ and $PT(ClO_4^-)$. A similar pattern apparently occurs also in the case of $PT(I_3^-)$, the EPR spectrum of which may be broadened owing to the strong spin–orbital interaction of the paramagnetic centres with the counterions.

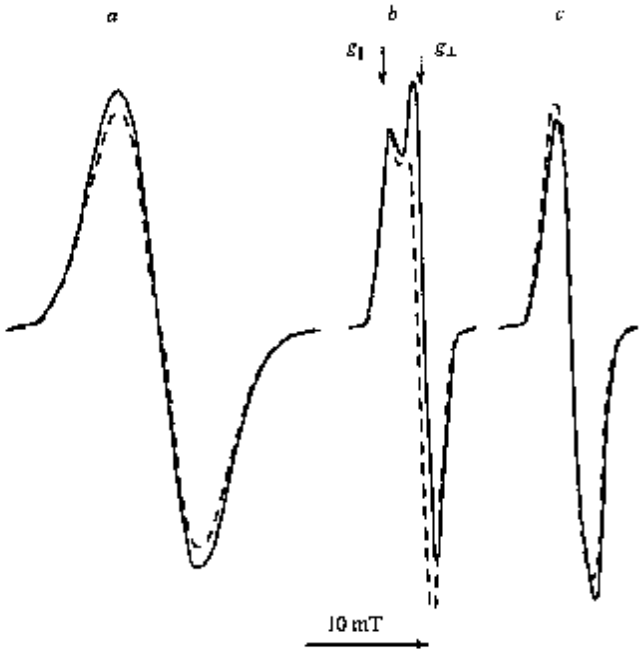

Figure 2. Typical 2 mm EPR absorption spectra of polythiophene synthesised electrochemically from thiophene and doped with I_3^- (*a*), BF_4^- (*b*), and ClO_4^- (*c*) anions. The spectra were recorded at $T = 300$ K (continuous line) and 200 K (dashed line).

Table 3 presents the magnetic resonance parameters calculated from the 2 mm EPR spectra, the d.c. and a.c. conductivities of the samples (σ_{dc} and σ_{ac}), and the energies of the excitation of an electron to the nearest level ($\Delta E_{\sigma\pi^*}$). Analysis of the data presented shows that, in the series of anions $I_3^- \rightarrow BF_4^- \rightarrow ClO_4^-$, the quantity $\Delta E_{\sigma\pi^*}$ increases by a factor greater than 4. This transition also leads to an increase in the conductivity of the film and to significant alteration of the concentration of paramagnetic centres. This may indicate charge transfer in PT both by polarons and by bipolarons, the ratio of the concentrations of which depends on the nature and number of the anions introduced into the polymer. The width of the PT spectral lines proved more sensitive to a change in the recording frequency, which indicates a less intense spin exchange in this polymer compared, for example, with PA[24, 31] and PPP.[25]

Table 3. The concentration of the paramagnetic centres (N), the electrical conductivity (σ_{dc}), the line width (ΔB_{pp}), the components of the g-tensor, and the energies of the excited electronic state ($\Delta E_{\sigma\pi^*}$) for polythiophene samples at $T = 300$ K.

Parameter	Polythiophene samples doped with the anions			
	I_3^-	BF_4^-	ClO_4^-	ClO_4^- [a]
$10^{-19}\,N$ / spins g^{-1}	2	8	5	10
$10^3\,\sigma_{dc}$ / S m^{-1}	0.5	1.2	16	61
ΔB_{pp} / mT				
3 cm band[b]	0.75(0.80)	0.23(0.34)	0.46(0.52)	0.70(0.25)
2 mm band	6.5	1.5	2.6	0.5
$g_\parallel$	2.00679[c]	2.00412	2.00230	2.00232[c]
$g_\perp$	2.00232[c]	2.00266	2.00239	2.00364[c]
$\Delta E_{\sigma\pi^*}$ / eV	1.6	4.0	7.0	4.5

[a] The sample was synthesised from bithiophene. [b] The values of ΔB_{pp} at 77 K are given in brackets. [c] Values calculated from the equation $\langle g \rangle = \frac{1}{3}(g_\parallel + 2g_\perp)$.

On reducing the temperature of the PT(BF_4^-) sample, a Dyson-like line is manifested in the perpendicular component of its EPR spectrum without an appreciable change in the signal intensity. The quantity A/B increases monotonically in the temperature range 100–300 K, which indicates an increase in the electrical conductivity of the sample σ_{ac}, as happens in classical low-dimensional semiconductors. Knowing the characteristic size of the polymer particles δ and using the relation $A/B(\delta)$, it is possible to estimate for amorphous low-dimensional semiconductors[32] the electrical conductivity of the sample and also the mobility μ and the rate of the 1D-diffusion of the charge carriers from the formula

$$\sigma_{ac} = N\mu e = \frac{Ne^2 \nu_{1,1D} c_{1,1D}^2}{kT}, \qquad (4)$$

where c_{1D} is the lattice constant. The quantities σ_{ac}, μ_{1D}, and ν_{1D} calculated for PT(BF_4^-) in this way were found to be respectively 3.6×10^2 S m^{-1}, 1.1×10^{-5} m^2 V^{-1} s^{-1}, and 3.2×10^{12} s^{-1} at room temperature.[30]

Polythiophene, synthesised from bithiophene and doped with ClO_4^- anions, is characterised by a single symmetrical EPR line at the 3 cm band, the width of which decreases monotonically from 0.7 to 0.25 mT on reducing the temperature from 300 to 77 K. In the 2 mm EPR band, this sample also shows a single line over a broad temperature range, which indicates the occurrence of charge transfer in it mainly by delocalised paramagnetic centres. With increase in temperature from 100 to 200 K ($T_c \approx 200$ K), the paramagnetic susceptibility of this sample decreases significantly and, on further rise of temperature, rises sharply (Fig. 3). This is accompanied by a corresponding change in line width, and the inverse relation of the functions $\Delta B_{pp}(T)$ and $\chi(T)$ (Fig. 3). This effect can be accounted for by the annihilation of polaron pairs to bipolarons when the temperature is varied from 100 K to T_c and on subsequent decomposition of the bipolaron into polarons at $T > T_c$, apparently owing to the intensification of the librations of the polymer chains. If one adopts a linear dependence of the rate of decomposition of bipolarons on the frequency of the librations of the polymer chains, then it is possible to estimate the activation energy for the latter process from the $\chi(T)$ behaviour. It proved to be $E_a \approx 0.16$ eV at $T > T_c$. Such polaron–bipolaron transformation is apparently in fact the cause of the unusual broadening, indicated above, of the EPR line of this sample at the 3 cm band, observed on raising the temperature.

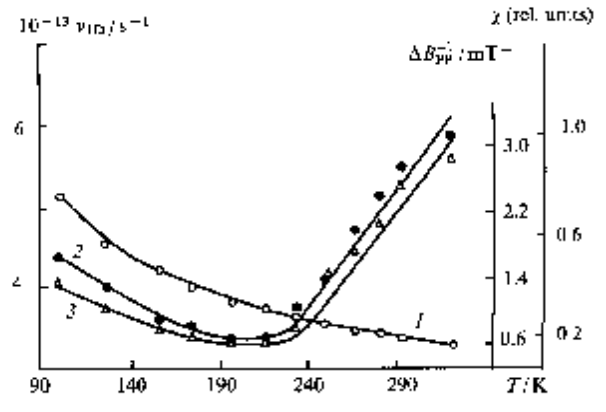

Figure 3. Temperature variations of the rate of diffusion of charge carriers ν_{1D} along a polymer chain (*1*), of the relative paramagnetic susceptibility χ (*2*), and of the inverse of the line width ΔB_{pp} (*3*) for polythiophene synthesised electrochemically from bithiophene and doped with ClO_4^- counterions.

As in the spectrum of polythiophene, a Dyson-like line appears in the EPR spectrum of polybithiophene at low temperatures, which reflects the change in the electrical conductivity of the film. Bearing in mind that the concentrations of the polarons and bipolarons are unchanged and using the above procedure, it is possible to determine the rate of 1D-diffusion of the charge carriers in the sample (Fig. 3). At room temperature, this quantity proved to be $\nu_{1D} = 3 \times 10^{13}$ s^{-1}, which is similar in order of magnitude to ν_{1D} determined for polarons in doped PANI,[33] in which the interchain charge transfer predominates. The weak temperature dependence of the rate of the 1D-diffusion of the charge carriers in bithiophene also indicates the predominance of the interchain charge transfer in this polymer and its increased dimensionality.

IV. Polypyrrole

Neutral PP is characterised by a complex spectrum at the 3 cm EPR band, consisting of a superposition of a narrow (0.04 mT) and a wider (0.28 mT) line with a g-factor ($g = 2.0026$) typical for π-conjugated and aromatic compounds.[15] The concentration of paramagnetic centres in neutral PP corresponds to one spin for several hundreds of monomer rings. The width and intensity of the narrow spectral line are of the activated character, whereas the wider component follows the Curie law. This indicates the existence in neutral PP of two types of paramagnetic centres with different relaxation parameters.

At the same EPR band, doped PP is characterised by an intense single and narrow line (~ 0.03 mT) with $g = 2.0028$, which obeys the Curie law in the temperature range 30–300 K.[15] The majority of the results obtained previously indicate that the charge carriers are not responsible for the EPR spectrum of this polymer because there are no correlations between the magnetic susceptibility and the concentration of charge carriers as well as between the line width and the mobility of the carriers. This may be interpreted as a result of the formation of spin-less bipolarons in PP during the doping of the latter. Thus the EPR signal of doped PP cannot yield adequate information about the conduction processes.

The spin probe method, based on the introduction of a stable nitroxyl radical into the test system, may prove more effective in this instance.[34] However, hitherto this method has been rarely used in the study of conducting polymers.[34, 35] The reason for this is primarily the fact that the low spectral resolution at $\nu_e \leqslant 10$ GHz precludes the separate recording of all components of the g- and A-tensors and hence hinders the separate determination of the magnetic parameters of the nitroxyl radicals and the paramagnetic centres localised on the polymer chains, as well as the establishment of the dipole–dipole interaction between different paramagnetic centres. Thus electrochemically synthesised PP, in which the nitroxyl radical was bound covalently to the pyrrole ring, has been investigated.[35] However, despite the appreciable concentration of the nitroxyl radicals introduced into the polymer, the 3 cm EPR spectrum of this sample showed no lines corresponding to the spin label.

The spin probe method proved to be more effective in the study of doped PP at the 2 mm EPR band.[36]

Fig. 4 presents the EPR spectra of 4-carboxy-2,2,6,6-tetramethyl-1-piperidinyloxyl (a nitroxyl radical), introduced as the probe and the counterion into a nonpolar model system and PP (electrochemically) simultaneously. The EPR spectrum of the spin-modified PP at the 3 cm band represents a superposition of the lines due to the probe, which is characterised by a rotational correlation time $\tau_c \geqslant 10^{-7}$ s, and a superimposed single line due to the paramagnetic centres (R) localised on the chain (Fig. 4*a*). This superposition of the individual spectra precludes the separate determination of the magnetic resonance parameters of the probe and the radical R in PP and also the analysis of the dipole–dipole broadening of their spectral components.

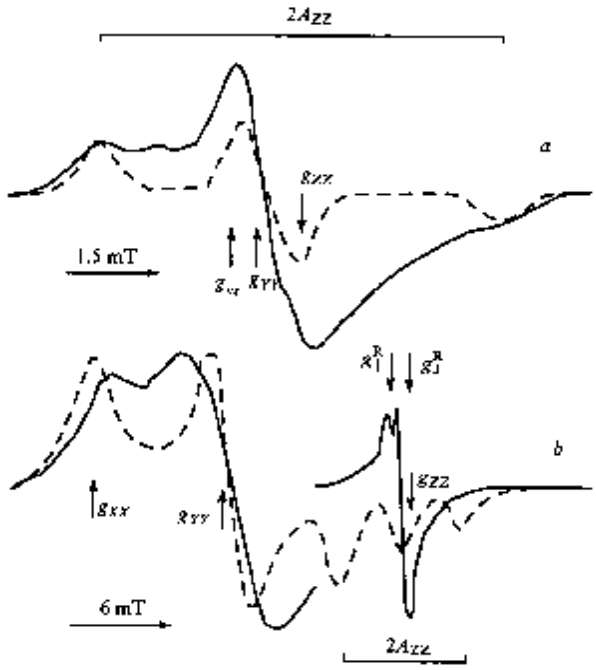

Figure 4. EPR absorption spectra of 4-carboxy-2,2,6,6-tetramethyl-1-piperidinyloxyl (a nitroxyl radical) introduced as a spin probe into frozen (120 K) toluene (dashed line) and conducting polypyrrole (continuous line). Recording band: (*a*) 3 cm; (*b*) 2 mm. Fig. (*a*) illustrates the anisotropic spectrum of the localised paramagnetic centres R as well as the measured magnetic parameters of the probe and the radical R.

The EPR spectrum of the spin-modified polymer systems at the 2 mm band has a higher information content (Fig. 4*b*). All the canonical components of the nitroxyl probe are fully resolved in the spectrum, which permits the direct determination of the principal values of its g- and A-tensors. Furthermore, in the region of the Z-component of the probe spectrum in PP, the axially symmetrical spectrum of the radical R is recorded with the magnetic parameters $g_{\parallel}^{R} = 2.00380$, $g_{\perp}^{R} = 2.00235$, and $\Delta B_{pp} = 0.57$ mT.

The form of the spectrum of this radical indicates its localisation on the polymer chain, i.e. charge transfer in PP by spin-less bipolarons, as happens in PPP(BF_4^-) and PT(BF_4^-). The difference $\Delta g = g_{\parallel}^{R} - g_{\perp}^{R} = 1.45 \times 10^{-3}$ corresponds to an excited electronic configuration in R with an excitation energy $\Delta E_{\sigma\pi^*} = 5.1$ eV, which is close to the excitation energy of the electron in neutral PPP.

The nitroxyl probe in nonpolar toluene is characterised by the following magnetic parameters: $g_{XX} = 2.00987$, $g_{YY} = 2.00637$, $g_{ZZ} = 2.00233$, $A_{XX} = A_{YY} = 0.6$, and $A_{ZZ} = 3.31$ mT. In the conducting PP, the quantity g_{XX} diminishes to 2.00906, whereas both the X- and Y-components of the probe spectrum are broadened by 4 mT (Fig. 4*b*). Analysis of the form of the probe spectrum permits the conclusion that there are no rapid movements of this radical in PP (correlation time $\tau_c \leqslant 10^{-7}$ s) even at comparatively high temperatures, which is apparently associated with the small size of the region of localisation of the probe, not exceeding 1 nm.

In neutral PP there are no fragments with an appreciable dipole moment. The dipole–dipole interactions between the radicals may be neglected, because the concentrations of the probe and the paramagnetic centres localised on the chain are small. The changes in the magnetic-resonance parameters of the probe on passing from the model nonpolar system to the conducting polymer matrix, indicated above, may occur as a consequence of the Coulombic interaction of the active fragment

of the probe and the spin-less charge carriers — bipolarons. The effective electric dipole moment of the bipolaron closest to the probe, calculated from the shift of the g_{XX} component, amounted to $\mu_v = 2.3$ D. The shift of the g_{XX} component of the probe g-factor may be calculated within the framework of the electrostatic interaction of the dipoles of the probe and the bipolaron by means of the following procedure. The potential of the electric field induced by the bipolaron at the location of the probe is defined by the expression [37]

$$E_d = \frac{kT}{\mu_u}(x\coth x - 1), \qquad (5)$$
$$x = \frac{2\mu_u\mu_v}{4\pi\varepsilon\varepsilon_0 kTr^3},$$

where μ_u is the electric dipole moment of the probe, ε and ε_0 are dielectric constants for the PP and the vacuum respectively, and r is the distance between the active fragment of the nitroxyl radical and the bipolaron. Using the variation of the increment in the isotropic hyperfine interaction constant for the probe due to the electrostatic field of the microenvironment $\Delta a = 7.3er_{NO}I^{-1}E_d$ (here r_{NO} is the distance between the N and O atoms of the active fragment of the probe and I is the resonance overlap integral for the C=C bond) as well as the relation $\partial g_{XX}/\partial A_{ZZ} = 2.3\times10^{-3}$ mT for 2,2,6,6-tetramethyl-1-piperidinyloxyl radicals,[21–23] it is possible to formulate the following equation for Δg_{XX}:

$$\Delta g_{XX} = 6\times10^{-3}\frac{er_{NO}kT}{I\mu_u}(x\coth x - 1). \qquad (6)$$

Adopting $\mu_u = 2.7$ D,[35] $\mu_v = 2.3$ D, and $r_{NO} = 0.13$ nm,[26] we obtain $r = 0.92$ nm.

The rate of spin–spin relaxation, which determines the width of the spectral line of the radical, can be formulated as $\tau_2^{-1} = \tau_{2(0)}^{-1} + \tau_{2(D)}^{-1}$ where $\tau_{2(0)}^{-1}$ is the rate of relaxation of a radical which does not interact with the environment and $\tau_{2(D)}^{-1}$ is the increment in the rate of relaxation due to the dipole–dipole interaction. The characteristic time of such interaction τ_c in a polycrystalline sample may be calculated from the broadening of the spectral lines $\delta(\Delta B_{X,Y})$.[39]

$$\tau_{2(D)}^{-1} = \gamma_e\delta(\Delta B_{X,Y}) \qquad (7)$$
$$= \frac{1}{2}\langle\Delta\omega^2\rangle[3J(0) + 5J(\omega_e) - 2J(2\omega_e)],$$

where

$$\langle\Delta\omega^2\rangle = \frac{1}{5}\left(\frac{\mu_0}{4\pi}\right)^2\gamma_e^4\hbar^2S(S+1)N\sum_{r_1}^{N}\sum_{r_2}^{N}\frac{(3\cos^2\theta-1)^2}{r_1^3r_2^3},$$

$$J(\omega_e) = \frac{2\tau_c}{1+\omega_e^2\tau_c^2}.$$

Here μ_0 is the magnetic permeability of a vacuum, $\hbar = h/2\pi$, $\omega_e = 2\pi\nu_e$ is the recording frequency, and θ is the angle between the vectors r_1 and r_2. The inequality $\omega_e\tau_c \gg 1$ holds for the majority of highly viscous condensed systems, so that, by averaging with respect to the angles $\Sigma\Sigma(3\cos^2\theta-1)^2(r_1^{-3}r_2^{-3}) = 6.8r^{-6}$ and, using the value $\gamma_e\delta(\Delta B_{X,Y}) = 7\times10^8$ s^{-1} and the value $r = 0.92$ calculated above, we obtain $\tau_{2(D)}^{-1} = \gamma_e\delta(\Delta B_{X,Y}) = 3\langle\Delta\omega^2\rangle\tau_c$ or $\tau_c = 8.1\times10^{-11}$ s. Bearing in mind that the average time between translational hops depends on the diffusion coefficient D and the average length of the hop, which is equal to the product of the lattice constant c_{1D} and the half-width of the spin delocalisation on the charge carrier $N_P/2$, i.e. $\tau_c = 1.5\langle c_{1D}^2N_P^2\rangle D^{-1}$, and, taking into account the value $D \approx 5\times10^{-7}$ m^2 s^{-1} typical for conducting polymers, we obtain $\langle c_{1D}N_P\rangle = 3$ nm, which corresponds approximately to four pyrrole rings. This quantity is close to the width of the bipolaron in polypyrrole and polyaniline, but is appreciably smaller than N_P obtained for polybithiophene.[40]

Thus the form of the EPR spectrum of the spin-modified PP, recorded at the 2 mm band, indicates extremely slow rotational motions of the probe, apparently as a consequence of the fairly dense packing of the polymer chains in PP. The interaction of the spin-less charge carriers with the active fragment of the spin probe leads to a redistribution of the spin density between the N and O atoms of the nitroxyl radical and hence to a change in its magnetic-resonance parameters. This makes it possible to determine the distance between the radical and the chain, along which the charge carrier moves, and also the effective length of the bipolaron in a randomly oriented polymeric semiconductor.

V. Polyaniline

A characteristic behaviour of polyaniline (PANI) is known [41] to be the insulator/conductor transition, occurring on protonation or oxidation of the polymer, i.e. on transition from its emeraldine base form (EB form) to the emeraldine salt form (ES form). This compound differs from other conjugated polymers in a number of features. Thus, in contrast to PPP, PT, and PP, both the benzene rings and the nitrogen atoms are involved in conjugation in PANI. On protonation or oxidation, the conductivity of the polymer increases by more than 10 orders of magnitude, whilst the number of electrons on the polymer chain remains unchanged.[42] Polyaniline in the EB form is an insulator. This form is amorphous and contains traces of the ES form, whereas the ES form of PANI contains highly conducting crystalline domains with a characteristic size of 5 nm [31] distributed in the amorphous EB phase.

The oxidation or protonation of the EB form of PANI is accompanied by a monotonic increase in the concentration of paramagnetic centres and a narrowing of the line from 0.2 to 0.05 mT in the 3 cm EPR spectrum.[28,43] The paramagnetic susceptibility of the weakly conducting PANI follows the Curie law, which indicates the formation of single polarons in the polymer chain, whereas Pauli spins, characteristic of the polaron lattice of a highly conducting polymer, have been detected in the ES form of PANI.[43,44]

The spin dynamics in PANI has been investigated by the complementary EPR and NMR spectroscopic methods.[45] The frequency dependences $\tau_{1n} \sim \omega_n^{1/2}$ (for nuclear spins) and $\Delta B_{PP}^{-1} \sim \omega_e^{-1/2}$ (for electron spins), obtained for isolated chains of the ES form of PANI, have been interpreted within the framework of the 1D-diffusion of polarons at a rate $\nu_{1D} > 10^{12}$ s^{-1}. The anisotropy of the spin diffusion ν_{1D}/ν_{3D} varies from 10^6 in the EB form to 10 in the ES form of PANI at room temperature. The correlation found between the spin dynamics and the charge transfer process has been interpreted as evidence in support of the predominantly interchain electron transport. However, this conclusion conflicts with another concept,[11,46] which predicts the 3D-transport of electrons in massive metal-like domains with a characteristic size 5 nm and 1D-transport of electrons between these domains. Investigations have shown that the charge transfer process in PANI is determined to a significant extent by structural parameters such as the crystallinity of the sample, the size of the crystalline domains, the conformation and degree of orientation of the chains, etc., which depend on the history of the sample and also on the amount of modifying agent introduced into it.

The results of studies on the magnetic and electrodynamic properties of PANI samples with different conductivities by 2 mm EPR spectroscopy are presented below.[18,47]

Fig. 5 presents the 2 mm EPR spectra of the initial and oxidised PANI samples. Analysis of these spectra showed that at least two types of paramagnetic centres were stabilised in the initial sample, namely an immobilised paramagnetic centre (R^1) (Fig. 5*a*) with the anisotropic magnetic-resonance parameters $g_{XX} = 2.00535$, $g_{YY} = 2.00415$, $g_{ZZ} = 2.00238$, $A_{XX} = A_{YY} = 0.33$, and $A_{ZZ} = 2.3$ mT, and a more mobile paramagnetic centre (R^2) with $g_\perp = 2.00351$ and $g_\parallel = 2.00212$. The relative

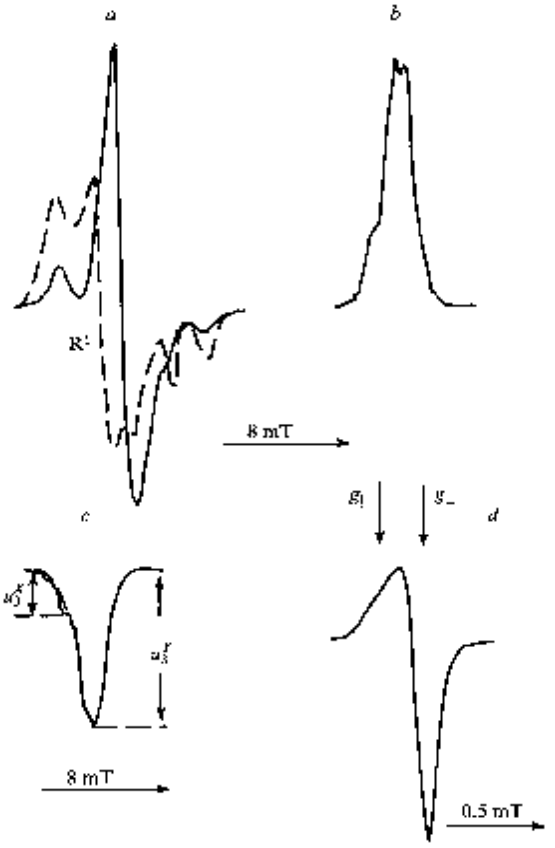

Figure 5. Typical 2 mm EPR absorption spectra (*a*, *d*) and the in-phase (*b*) and $\pi/2$ out-of-phase (*c*) components of the dispersion signal of neutral ($z = 0$) and oxidised ($z = 0.53$) (*d*) polyaniline recorded at $T = 300$ K. The dashed lines represent the absorption spectrum of the radical R^1 (*a*) localised on the chain and the $\pi/2$ out-of-phase component of the dispersion signal of the neutral sample at $T = 200$ K (*c*).

concentrations of these radicals N_i depend both on the degree of oxidation and on the temperature of the sample (Fig. 6*a*). The concentrations of paramagnetic centres of both types increase with increasing z (Table 4), which can be accounted for by an increase in the number of spin charge carriers and by the formation of a polaron lattice in PANI for $z \geqslant 0.3$.

The paramagnetic centre R^1 with an anisotropic EPR spectrum can be attributed to the radical species $(-C_6H_4-NH-C_6H_4-)^{\cdot}$ localised on the polymer chain. Its magnetic parameters differ somewhat from those of the structurally similar radical $-C_6H_4-N-C_6H_4-$.[26] This is apparently associated with a lower degree of localisation of the unpaired electron on the nitrogen atom ($\rho_N^{\pi} = 0.39$) and with a more planar conformation of the latter radical. The contribution of the CH groups of the radical to g_{xx} is small ($g_{xx} \approx 1.7 \times 10^{-5}$, see Buchachenko and Vasserman[26]), so that it can be neglected. The energies of the excited electronic configurations of the radical R^1 are $\Delta E_{n\pi^*} = 3.8$ eV and $\Delta E_{\sigma\pi^*} = 6.5$ eV for $\rho_N^{\pi} = 0.61$.[48]

The averaged g-factor of the radicals $R^1(g) = \frac{1}{3}(g_{xx} + g_{yy} + g_{zz})$ is close to the isotropic g-factor $R^2(g) = \frac{1}{3}(2g_{\perp} + g_{\parallel})$ for the paramagnetic centres R^2. The polaron diffusing along the polymer chain at an effective rate $\nu_{1D}^0 \geqslant 10^5$ s^{-1} [see Eqn (2)] may therefore be responsible for the EPR spectrum of the radical R^2.

During the oxidation of the initial PANI sample, the perpendicular component of the EPR spectrum becomes monotonically narrower and the paramagnetic susceptibility increases (Table 4) before the attainment of the degree of oxidation $z = 0.53$, which constitutes additional evidence for the formation in the highly conducting PANI of regions with a high spin density and rapid spin–spin exchange. This fact as well as the decrease in the g-factor for the radical R^2 with increase in z may be associated with the decrease in the spin density on the nucleus of the nitrogen atom and the change in the conformation of the polymer chains. The C–N–C bond angle in PANI is known[1] to increase by 22° on passing from the ER to the ES form. Calculation shows that this may alter $g_{\perp}$ only by several per cent. A more significant change in this magnetic parameter is induced by a change in the dihedral angle θ, i.e. the angle between the planes of neighbouring benzene rings. Taking into account the dependence of the overlap integral of the p_z orbitals of the nitrogen atoms and the carbon atom of the PANI benzene ring in the *para*-position relative to the

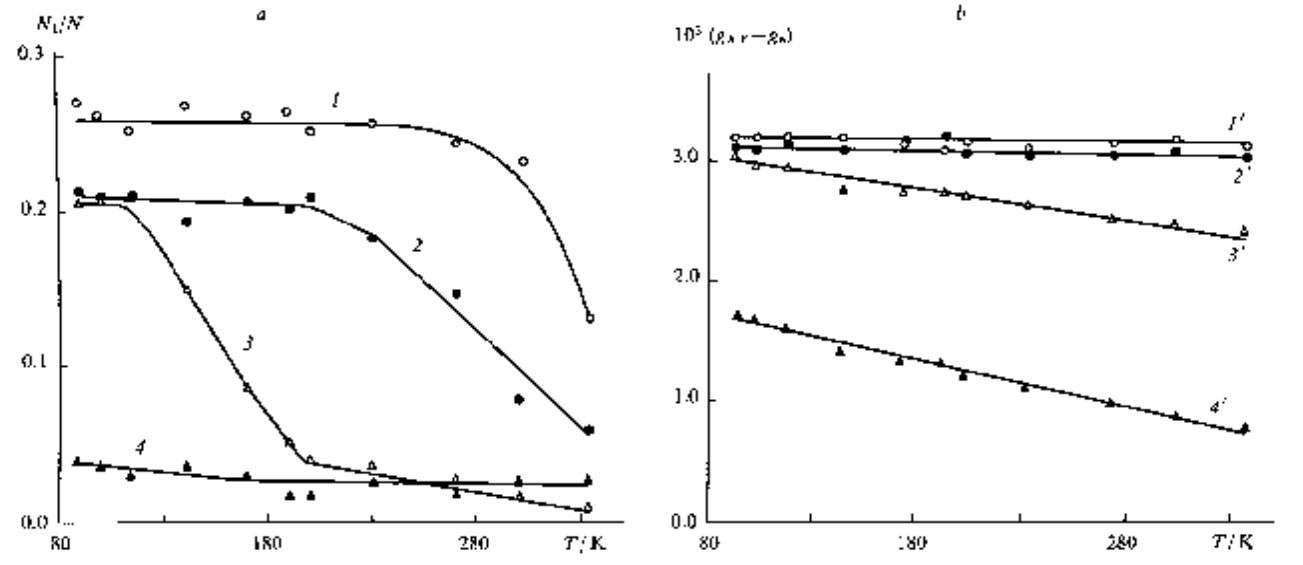

Figure 6. Temperature variations of the relative concentration N_i/N (*a*) and the g_{xx}-factor (*b*) of the paramagnetic centres R^1 localised in polyaniline with different degrees of oxidation z: (*1*) and (*1'*) 0; (*2*) and (*2'*) < 0.01; (*3*) and (*3'*) 0.02; (*4*) and (*4'*) 0.2.

Table 4. Dependence of the electrical conductivity (σ_{dc}), the critical temperature (T_0), the Pauli susceptibility (χ_P), the density of states at the Fermi level [$n(\varepsilon_F)$], the distance between the polaron level and the Fermi level (Δ_3), the polaron localisation length (L), the concentration of paramagnetic centres (N), the line width (ΔB_{PP}), and the spin–spin relaxation time (τ_2) for polyaniline samples at $T = 300$ K on their degree of oxidation z.

Parameter	Degree of oxidation z							
	0.00	0.01	0.02	0.06	0.20	0.30	0.39	0.53
σ_{dc}/S m^{-1}	$5\cdot10^{-6}$	$6\cdot10^{-6}$	$1\cdot10^{-4}$	$2\cdot10^{-2}$	100	270	560	1780
$10^{-4}\,T_0$/K	–	14	–	–	1.2	–	0.97	0.18
$10^6\,\chi_P$	~0.8	3	–	–	51	–	86	101
$n(\varepsilon_F)$/eV^{-1} mol^{-1}	0.04	0.09	–	–	1.6	–	2.7	3.2
Δ_3/eV[a]	–	0.04	–	–	0.33	–	0.52	0.61
L/nm	–	0.2	–	–	1.1	–	1.2	6.8
$10^{-19}\,N$/spins g^{-1}	1.0	1.2	3.2	4.7	22	55	91	195
$10^3\,\tau_2$/s[b]	0.62	0.64	0.82	2.3	5.2	4.5	5.0	15.0
ΔB_{PP}/mT								
3 cm band	1.06	1.02	0.80	0.28	0.125	0.145	0.125	0.039
2 mm band	1.50	1.45	1.31	–	0.60	–	0.29	0.162

[a] The values of Δ_3 were calculated by the formula $\Delta_3 = 0.5\,\hbar^2\,(3\pi^2 N)^{2/3}\,m_e^{-1}$. [b] The times τ_2 were calculated by the formula $\tau_2^{-1} = 0.866\gamma_e\Delta B_{PP}$.

nitrogen atom on the dihedral angle ($I \sim \cos\theta$)[13] and assuming that $\theta = 56°$ for the initial EB,[49] it is possible to calculate the effective dihedral angle and the spin density on the nitrogen atom in the ES form of PANI with $z = 0.2$, which are respectively $\theta = 33°$ and $\rho_N^\pi = 0.42$. The decrease in the angle θ leads to an increase in the transfer integral and hence to a greater delocalisation of the unpaired electron over the benzene rings. Thus the change in the magnetic parameters on oxidation of PANI reflects the transition to a more planar chain conformation.

It is important to note that the shape of the EPR spectrum of the radical R^2 in the ES form of PANI with $z = 0.2$ undergoes major change at 300 K. Whereas the inequality $g_\perp > g_\parallel$ is valid for this sample when $z < 0.2$ and $T \leqslant 300$ K, the inequality $g_\parallel > g$ actually holds when $z = 0.2$ and $T \geqslant 300$ K (Fig. 5). The latter inequality remains unaltered for $z \geqslant 0.2$ in the temperature range $90 \leqslant T \leqslant 330$ K. We recorded a similar transformation of the spectrum previously[50] on saturation of a PANI sample with water vapour and explained it by a significant change in the conformation of the radical R^2 as a consequence of the formation of H_2O bridges between the polymer chains. On the other hand, in the case described the change in line shape can be accounted for by the transformation of the polymer chains.

The components of the hyperfine structure, arising as a consequence of the interaction of the unpaired electron with the protons of the neighbouring benzene rings, have also been recorded in the EPR spectra of PANI samples with $z \geqslant 0.3$. The isotropic hyperfine interaction constant a_H is correlated with z and varies in the range 5.0–9.6 μT for different samples, which corresponds to a spin density $\rho_H^\pi = (2.2-4.3)\times10^{-4}$. The density of the unpaired electron delocalised over two benzene rings in a solution of the EB form of PANI in dioxane is $\rho_H^\pi = 1.5\times10^{-2}$.[48] The data obtained therefore indicate the delocalisation of the unpaired electron over a larger number of benzene rings owing to the more planar conformation of the ES samples investigated.

Bell-like components with a Gaussian distribution of the spin packets (Figs 5*b* and 5*c*), the intensity and shape of which depend on the amplitude B_m and the frequency ω_m of the high-frequency modulation, the amplitude of the magnetic component of the radiofrequency field B_1, and also on the spin–spin (τ_1) and spin–lattice (τ_2) relaxation times of the paramagnetic centres, have been recorded in the 2 mm EPR spectra of PANI samples. The appearance of such signals is induced by the effect associated with the rapid adiabatic passage of an inhomogeneously broadened line,[27] which may be accounted for as follows.

The shape of an individual spin packet in PANI is determined by the time parameters τ_1, τ_2, $(\gamma_e\Delta B_{PP})^{-1}$, ω_m^{-1}, $(\gamma_e B_m)^{-1}$, $(\gamma_e B_1)^{-1}$, and $B_1(dB_0/dt)^{-1}$. The distance between the spin packets which have moved apart is $A\omega_H$ and varies linearly with the recording frequency. On transition to stronger magnetic fields, the frequency ν_{ex} of the spin exchange between the paramagnetic centres with $S = -\frac{1}{2}$ and $g \approx 2$, separated by a distance r, decreases in accordance with the law[51]

$$\nu_{ex} \sim \frac{4\mu_B^2}{r^3}\exp\left[\frac{-0.25B_0^2r^6}{\mu_B^2}\right],$$

as a consequence of which the interaction between the spin packets diminishes and their width begins to depend on the recording frequency.[52]

$$\Delta B_{PP} = \Delta B_{PP}^0 + \frac{\Delta\omega_H^2}{8\nu_{ex}}. \tag{8}$$

In the adiabatic passage of a saturated signal [i.e. when $\gamma_e\omega_m B_m \ll \gamma_e^2 B_1^2$ and $s = \gamma_e B_1(\tau_1\tau_2)^{1/2} \geqslant 1$, where s is the EPR signal saturation factor], a stationary trajectory of the paramagnetic centre magnetisation vector is established and the succeeding signal projections, for example the dispersion U,[53] with the shape function $g(\nu_e)$ are recorded on the X, $-Y$, and $-X$ axes.

$$U = a_1 g'(\nu_e)\sin(\omega_m t) + a_2 g(\nu_e)\sin(\omega_m t - \pi) + a_3 g(\nu_e)\sin(\omega_m t \pm \tfrac{1}{2}\pi). \tag{9}$$

The inequality $\omega_m\tau_1 \gg 1$ is obtained for the EB form of PANI, so that the dispersion signal is determined mainly by the last two terms of Eqn (9). In this case the relaxation times may be determined from the central amplitude of these components by means of the following formulae:[54]

$$\tau_1 = \frac{3\omega_m(1+6\Omega)}{\gamma_e^2 B_{10}^2\Omega(1+\Omega)}, \tag{10a}$$

$$\tau_2 = \frac{\Omega}{\omega_m}, \tag{10b}$$

where $\Omega = a_3 a_2^{-1}$ and B_{10} is the value of B_1 for $a_1 = -a_2$.

In the EPR spectra of the ES form of PANI, the passage effects are less appreciable and the relaxation times can therefore be calculated from the formulae[54]

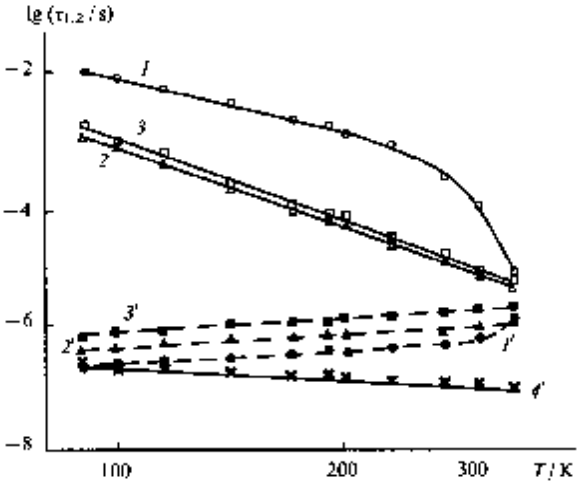

Figure 7. Temperature variations of the effective spin–lattice (τ_1) (curves *1–3*) and spin–spin (τ_2) (curves *1'–4'*) relaxation times of the paramagnetic centres in polyaniline with different degrees of oxidation z: (*1*) 0; (*2*) < 0.01; (*3*) 0.02; (*4*) 0.2.

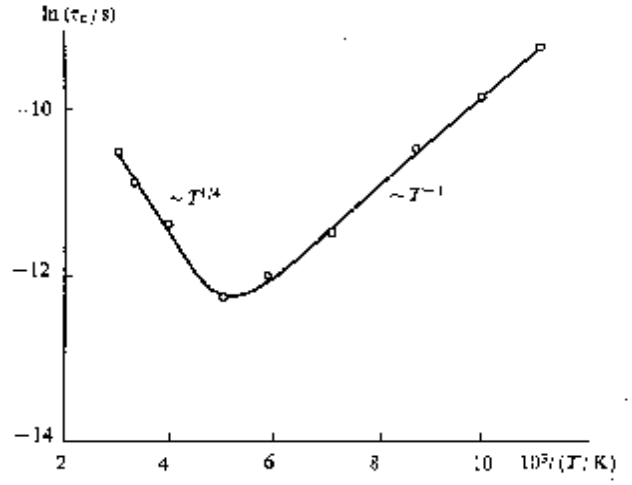

Figure 8. Arrhenius plot for the correlation times τ_c of the anisotropic librations of the polymer chains in the EB form of polyaniline with the degree of oxidation $z = 0$.

$$\tau_1 = \frac{\pi a_3}{2\omega_m a_1}, \tag{11a}$$

$$\tau_2 = \frac{\pi a_3}{2\omega_m (a_1 - 1/a_2)}. \tag{11b}$$

Fig. 7 presents the temperature variations of the effective relaxation times of the paramagnetic centres in different PANI samples. Evidently the spin–lattice relaxation time diminishes with increase in z, which indicates an increase in the number and size of the quasi-metallic domains in the ES form of PANI. It also follows from the figure that a temperature dependence of the type $\tau_1^{-1} \sim NT^l$, where $l = 3-4$ for $z \leqslant 0.02$ and $l = 0.3$ for $0.02 < z \leqslant 0.20$, is characteristic of PANI, which is a consequence of the sharp change in the rate of energy transfer from the spin ensemble to the polymer lattice and a change in the mechanism of charge transport during the oxidation of PANI.

The times τ_1 and τ_2 are effective and are determined by the relaxation times of the localised and mobile paramagnetic centres — the radicals R^1 and R^2 at the concentrations N_1 and N_2 respectively — so that for the general case one can write

$$N\tau_{1,2}^{-1} = N_1(\tau_{1,2}^{-1})_{loc} + N_2(\tau_{1,2}^{-1})_{mob}, \tag{12}$$

where $N = N_1 + N_2$. This equation permits the separate determination of the relaxation parameters of the trapped and mobile paramagnetic centres in the polymer.

We shall now consider the possibility of using the 2 mm EPR spectroscopic method for the investigation of the dynamics of the polymer chains in PANI and other conducting polymers in which the paramagnetic centres exhibit an appreciable anisotropy of the magnetic parameters. It is seen from Fig. 6*b* that the quantity g_{xx} for the radical R^1 depends in a complex manner on the degree of oxidation z and the temperature of PANI. The decrease in this parameter with increase in z and/or temperature may be explained both by the increase in the polarity of the microenvironment of the radical R^1 and by the acceleration of the small-scale vibrations of the polymer chain and hence of the radical localised on the latter. The motions of the macromolecules in this and other similar polymers are anisotropic and are characterised by a correlation time $\tau_c \geqslant 10^{-7}$ s.[54,55] The 'linear' EPR absorption spectra are usually insensitive to superslow motions and such molecular processes are therefore better investigated by the RF-saturation transfer method (ST-EPR).[56]

The ST-EPR method is based on the introduction into the test system of a nitroxyl label or probe and the recording of the spectrum of this radical under the conditions of the rapid passage of the saturated signal. On rotation of the paramagnetic centres, the above conditions may not be fulfilled for spin packets oriented in a particular way relative to the direction of the external magnetic field, as a result of which the form of the overall spectrum changes. It had been shown earlier[23] that the parameter most sensitive to the anisotropy of the molecular dynamics is the ratio of the components of the derivative of the dispersion signal, $K_{anis} = a_3^X/a_3^Y$, $\frac{1}{2}\pi$ out-of-phase. The sensitivity of the ST-EPR method also depends on the anisotropy of the magnetic parameters of the paramagnetic centres and on the recording frequency.[56] Bearing in mind that the paramagnetic centres localised on the polymer chain are themselves paramagnetic labels and are characterised by an appreciable anisotropy of the magnetic parameters, one may expect an increase in the effectiveness of this method in the study of conducting compounds at the 2 mm EPR band.

As can be seen from Fig. 5*c*, the parameter K_{anis} increases with increase in the temperature of the sample. This is a result of the anisotropic librational reorientations of the pinned polarons around the specified X axis of the polymer chains. The correlation time for the librations of the chains, calculated from the ST-EPR spectra by the method described by the present author,[21–23] was found to be given by the following expression for the initial PANI sample.

$$\tau_c = 2.4 \times 10^{-7} \exp\left(\frac{0.046}{kT}\right) \text{s},$$

in the temperature range $200 \leqslant T \leqslant 90$ K (Fig. 8). At higher temperatures, the correlation time varies in accordance with the law

$$\tau_c(T) = 61.1 \exp\left[-\left(\frac{T_0}{T}\right)^{1/4}\right] \text{s},$$

where

$$T_0 = \frac{18.1}{kn(\varepsilon_F)L^3} = 1.5 \times 10^7 \text{ K}.$$

Here T_0 is the percolation constant, which depends on the density of states $n(\varepsilon_F)$ on the Fermi level ε_F and L is the charge carrier localisation length. Using $n(\varepsilon_F) = 4.5 \times 10^{-2}$ eV^{-1} mol^{-1}, it is possible to obtain the polaron localisation length in neutral PANI, which is 0.53 nm, and the most probable length of the 3D-hop of the polaron between the chains $R = 0.39L(T_0/T)^{1/4} = 3.1$ nm at

$T = 300$ K. The data obtained indicate a close relation between the molecular spin dynamics in the EB form of PANI. With increase in τ_e or with significant decrease in B_1, the ST-EPR spectrum becomes insensitive to the molecular dynamics and in this case $K_{mov} \approx 0.07$. The maximum value of τ_c recorded at the 2 mm EPR band can be estimated from these data as $\sim 10^{-4}$ s at 90 K.

We shall now consider the dynamic parameters of the polaron in PANI. As in the case of a mobile soliton in *trans*-polyacetylene,[24] the diffusion of the polaron along the polymer chain is characterised by a translational propagator of motion $P_{ij}(r, r_{ij}, \tau)$. This quantity determines the probability at a time $t = \tau$ that the ith spin is located in the region $r + dr$ relative to the new position of the jth spin, which was located in the initial instant at the point r_{ij} relative to the ith spin.

On solving the equation for Brownian diffusion

$$\frac{\partial P_{ij}(r, r_0; \tau)}{\partial t} = \mathbf{D}_{ij} \Delta P(r, r_0; \tau), \qquad (13)$$

we find the propagator for a diffusing polaron subject to the initial condition $P_{ij}(r, r_0, \tau) = \delta(r_0 - r)$, where $\mathbf{D}_{ij} = [D_i]$ and $\mathbf{i}$ is the unit vector for the molecular coordinate system. For a 1D-system, the above propagator is defined explicitly by the relation [39]

$$P(r, r_{ij}, \tau)_{1D} = (4\pi\nu_{1D}\tau)^{1/2} \exp\left[-\frac{(r - r_0)^2}{4\nu_{1D}c_{1D}^2\tau}\right] \exp(-\nu_{3D}\tau). \quad (14)$$

The mobile polaron induces a local magnetic field $B_{loc}(t)$ at the location of other electron or nuclear spins, influencing thereby the relaxation times of the latter. The relaxation time can therefore be expressed in terms of the frequency function $\tau_{1,2} = f[J(\omega)]$, where

$$J(\omega) = \int_{-\infty}^{+\infty} G(\tau) \exp(-i\omega\tau) d\tau.$$

Here $J(\omega)$ is the spectral density function. The autocorrelation function of a local field $B_{loc}(t)$ fluctuating in a discrete system is

$$G(\tau) = c_{1D} \sum_{r_0}^{n} \sum_{r}^{n} A(r_0, t) P(r, r_0; \tau) F(r_0) F^*(r) dr_0 dr, \qquad (15)$$

where $A(r,t)$ is the probability that the spin is at a distance r at time t and is equal to the spin concentration N, while $F(r)$ is the probability that two spins are at a distance r at time t. For frequencies $\omega \ll \nu_{1D} c_{1D}^2 (r - r_0)^{-2}$ the spectral density function assumes the form:[37]

$$J(\omega) = N J_{1D}(\omega) \sum \sum F(r_0) F^*(r) f_{1D}(|r - r_0|), \qquad (16)$$

where $N = N_1 + (1/\sqrt{2})N_2$ is the probability that in the initial instant the spin is in the position r_1, $J_{1D}(\omega) = (2\pi\nu_{1D}\nu_e)^{-1/2}$ for $\nu_{3D} \ll \nu_e \ll \nu_{1D}$ and $J_{1D}(\omega) = (2\pi\nu_{1D}\nu_{3D})^{-1/2}$ for $\nu_{3D} \gg \nu_e$, $F(r_0)F^*(r)f_{1D}(|r - r_0|) = (3\cos^2\vartheta - 1)^2 r_1^{-3} r_2^{-3}$, and ϑ is the angle between the vectors $\mathbf{r}_1$ and $\mathbf{r}_2$.

The relaxation times of the paramagnetic centres in PANI are characterised by the relation $\tau_{1,2} \sim N\omega_e^{-1/2}$,[45,46] so that the experimental results presented in Fig. 7 may be interpreted within the framework of the modulation of the spin relaxation of the 1D-diffusion of a polaron and its interchain hopping 3D-transfer at rates ν_{1D} and ν_{3D} respectively. Since the electron relaxation is determined mainly by the dipole–dipole interaction between equivalent electron and nuclear spins, it follows subject to the condition $S = I = \frac{1}{2}$, that the equations for the rate of relaxation [39] in the polycrystalline sample can be more simply formulated:

$$\tau_1^{-1} = \frac{1}{5}(\Delta\omega^2)[J(\omega_e) + 4J(2\omega_e)] \qquad (17a)$$

$$= 1.16 \times 10^{-42} N (\nu_{1D})^{-1/2} \sum \sum_i,$$

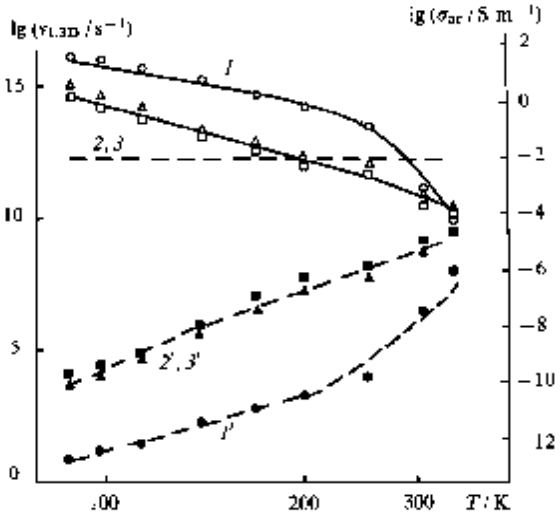

Figure 9. Temperature variations of the rates of diffusion of the polarons along the chain (ν_{1D}) and between the chains (ν_{3D}) in polyaniline with the degrees of oxidation $z = 0$ (*1*), ≈ 0.01 (*2*), and 0.02 (*3*) and also of the electrical conductivity σ_{ac} calculated within the framework of the isoenergetic (continuous lines) and activated (dashed lines) interchain charge transfer. The horizontal line corresponds to the effective value ν_{3D} calculated by Eqns (16) and (17) subject to the condition $\tau_1 \approx \tau_2$ for polyaniline with $z \geq 0.3$.

$$\tau_2^{-1} = \frac{1}{2}(\Delta\omega^2)[3J(0) + 5J(\omega_e) + 2J(2\omega_e)] \qquad (17b)$$

$$= 4.13 \times 10^{-38} (\nu_{1D})^{-1/2} [(\nu_{3D})^{-1/2} + 2.28 \times 10^{-6}] \sum \sum_i,$$

where $\Sigma\Sigma_i$ is the lattice sum equal to 1.21×10^{57} m^{-6} for PANI.

Fig. 9 presents the temperature variations of the rates of diffusion ν_{1D} and ν_{3D} of the paramagnetic centres in certain PANI samples under the conditions of spin delocalisation over five monomer units. Evidently the anisotropy of the spin dynamics is a maximum in the initial sample (EB form) and diminishes with increase in the degree of oxidation z. For comparatively high degrees of oxidation ($z \geq 0.2$), the times τ_1 and τ_2 are approximately equal and depend only slightly on temperature in view of the intense spin–spin exchange in the metal-like domains and the increased dimensionality of the system. Bearing in mind that $\tau_2^{-1} \approx \tau_1^{-1}$ it is possible to calculate ν_{3D}. It proved to be 1.6×10^{12} s^{-1} for PANI samples with $z \geq 0.2$ (Fig. 9). The calculated values of ν_{1D} are significantly smaller than the rate of 1D-diffusion of the polaron, obtained for PANI by magnetic-resonance methods in weak recording fields.[45]

It had been shown earlier [43] that the anisotropy of the spin diffusion in PANI at room temperature remains fairly high up to $z \approx 0.6$, but it follows from Fig. 9 that the ratio ν_{1D}/ν_{3D} remains fairly high only in neutral and weakly oxidised samples. The dimensionality of PANI increases on oxidation as a result of the intensification of the interaction between the polymer chains, so that the spin diffusion in this polymer becomes almost isotropic for $z \geq 0.2$, which is characteristic of classical 3D-semiconductors. This finding constitutes unambiguous evidence for the formation of massive quasi-metallic domains in the oxidised polymer and for the increase in its dimensionality and crystallinity, which we confirmed in an X-ray diffraction study of PANI.[47] During the oxidation of the polymer, the concentration of electron traps diminishes, which decreases the probability of the scattering of electrons by lattice phonons and hence leads to a weaker temperature dependence of the relaxation and dynamic parameters of the charge carriers in PANI, as happens in classical inorganic amorphous semiconductors.[39]

If one assumes that the diffusion coefficients D of the spin and diamagnetic charge carriers are identical, it is possible to obtain from Eqn (4) the quantity σ_{1D}, which is 10 S m^{-1} for the sample with $0 \leqslant z \leqslant 0.02$ at room temperature whereas σ_{3D} increases in this range of z from 1.0×10^{-3} to 0.5 S m^{-1}. Subject to the condition $\nu_{1D} \approx \nu_{3D}$, these quantities are $\sigma_{1D} = (5-18)\times10^{3}$ and $\sigma_{3D} = (3-10)\times10^{3}$ S m^{-1}. Thus the rate of the interchain charge transfer increases with increase in z, which constitutes additional confirmation of the increase in the number and size of the quasi-metallic 3D-domains in PANI.

As in other quasi-one-dimensional polymeric semiconductors, different charge transfer processes may occur in PANI, such as charge transfer along a π-conjugated chain as well as the interchain and interfibrillar charge transfer. Evidently the contribution of each of these processes to the bulk conductivity depends on the method of synthesis, structure, and degree of oxidation of the polymer and also on the dynamics of the nonlinear excitations.

The data obtained at the 2 mm EPR band permit a more correct and fuller determination of the mechanism of the charge transfer in PANI. As shown above, the EB form of PANI exhibits a strong temperature dependence of the spin–lattice relaxation time. This means that the hops of the unpaired electron in PANI are accompanied by the absorption or emission of a minimal number of polymer lattice phonons. Since the linkage between the spin and the lattice in the EB form of PANI is fairly strong, multiphonon charge transfer processes predominate in this system. The approach proposed for the description of the motion of solitons in lightly doped *trans*-PA may therefore be used in the study of the spin dynamics in the amorphous regions of PANI.[60]

The essential feature of this approach consists in the phonon-linked interchain tunnelling of the charge between isoenergetic levels of the carriers under the conditions of Coulombic interaction of a soliton with a charge q_1 and an ion with the opposite charge q_2. The excess charge $\Delta q = q_1 - q_2$ may undergo a phonon-linked transfer, with a finite probability, to a neutral carrier moving along a neighbouring polymer chain. If in the instant of such transfer the charge carrier is also in the vicinity of the ion, then its energy before and after charge transfer remains unchanged. In this case, the components of the electrical conductivity of the polymer, in which the charge is transferred between soliton levels, are determined by the probability that the soliton is located near a charged ion and also by the probability that the energies of the charge carriers are within the limits of kT,

$$\sigma_{dc} = \frac{k_1 e^2 \gamma(T) \xi N_0}{kTR_0} \exp\left(\frac{-2k_2 R_0}{\xi}\right) = \sigma_0 T^n, \tag{18a}$$

$$\sigma_{ac} = \frac{e^2 N_i^2 N_0 \xi_\parallel^3 \xi_\perp^2 \nu_e}{384kT} \left[\ln\frac{2\nu_e}{N_0\gamma(T)}\right]^4 = \sigma_0 \nu_e T^{-1} \left[\ln\frac{k_3\nu_e}{T^{n+1}}\right]^4, \tag{18b}$$

where $k_1 = 0.45$, $k_2 = 1.39$, and k_3 are constants. $\gamma(T) = \gamma_0 (T/300)^{n-1}$ is the hopping frequency of the charge carrier, $\xi = (\xi_\parallel \xi_\perp^2)^{1/3}$, $\xi_\parallel$ and $\xi_\perp$ are the averaged parallel and perpendicular lengths of the charge carrier respectively, $N_0 = N_n N_{ch} (N_n - N_{ch})^{-2}$ (N_n and N_{ch} are the numbers of the neutral and charged carriers per monomer unit respectively), and $R_0 = [(\frac{4}{3}\pi N_i)]^{-1/3}$ is the typical distance between ions at a concentration N_i. The above temperature variations have been obtained experimentally for lightly doped *trans*-PA[61,62] and other conducting polymers.[63,64] It can be shown that, within the framework of the approach considered, the following relation is valid:

$$\frac{\sigma(\nu_e \to \infty)}{\sigma(\nu_e \to 0)} = \frac{\exp(1.9k_1)}{k_1^4}, \tag{19}$$

where $k_1 = (0.4\pi N_i \xi_\parallel \xi_\perp^2)^{1/3}$ is a constant. Calculation showed that $\sigma_{ac}/\sigma_{dc} \approx 130$ for PANI at $\nu_e = 140$ GHz.

It is essential to note that the approach described is valid in the case of charge transfers by carriers with a small radius such as solitons. This approach may also be used for the interpretation of the spin dynamics in other conjugated polymers,[64] for example in tetrathiafulvalene (see below), where charge transfer is effected by nonlinear excitations with a small radius.[65] Apparently it can also be used for the interpretation of the spin dynamics in PANI when there are N_n polarons with a charge q and N_{eh} bipolarons with a charge $2q$ in this polymer.

Fig. 9 presents the temperature dependence of the electrical conductivity σ_{ac} calculated from Eqn (18b) by using $n = 12.9$ and $\sigma_0 = 2.8\times10^{-12}$ S m^{-1} s K for the initial sample in the EB form and $n = 12.6$ and $\sigma_0 = 8.8\times10^{-14}$ S m^{-1} s K for the sample with $0.02 \geqslant z \geqslant 0$, as well as $k_3 = 1\times10^{-4}$ s K^{n+1}. A satisfactory agreement of the experimental $\nu_{1D}(T)$ and theoretical $\sigma_{ac}(T)$ relations obtained for these samples follows from the figure. Bearing in mind that the conductivity of PANI obeys the law $\sigma_{dc}(T) \sim T^n$ ($n = 12$ - 20) for a low oxidation level],[47] one may conclude that the charge transfer mechanism considered operates in PANI with $z \leqslant 0.02$.

An appreciable temperature dependence of σ_{ac} may also be observed on thermal activation of the charge carriers with an energy E_a for activation from their energy level located in the gap to the conductivity band. In this case the conductivities σ_{dc} and σ_{ac} can be determined from the equations [6]:

$$\sigma_{dc} = \sigma_0 \exp\left(-\frac{E_a}{kT}\right), \tag{20a}$$

$$\sigma_{ac} = \sigma_0 \nu_e^{\gamma} T \exp\left(-\frac{E_a}{kT}\right), \tag{20b}$$

where γ is a constant which varies in the range $0.3 < \gamma < 0.8$ depending on the dimensionality of the system. Indeed the $\nu_{3D}(T)$ relations can be fitted by the function $\sigma_{ac}(T)$ calculated from Eqn (20b) with $\gamma = 0.8$ and $\sigma_{ac}^0 = 3.2\times10^{-18}$ S m^{-1} s$^{0.8}$ K^{-1} and $E_a = 0.06$ eV at $T \leqslant 240$ K or $\sigma_{ac}^0 = 9.1$ S m^{-1} s$^{0.8}$ K^{-1} and $E_a = 0.9$ eV at $T \geqslant 240$ K for the sample in which $z = 0$ and with $\sigma_{ac}^0 = 1.4\times10^{-11}$ S m^{-1} s$^{0.8}$ K^{-1} and $E_a = 0.13$ eV for samples in which $0.02 \geqslant z > 0$ (Fig. 9). However, the function $\sigma_{dc}(T)$ for the initial sample has a higher slope than should follow from Eqn (20b). Therefore the activation mechanism of charge transfer can apparently be realised in a polymer with an intermediate degree of oxidation.

The temperature dependence of the electrical conductivity of PANI with $z \geqslant 0.2$ obeys the law $\sigma_{dc} = \sigma_0 \exp[-(T_0/T)^{1/2}]$.[47] This is evidence for charge transfer in the oxidised PANI within the framework of the variable range hopping model.[66] In this case, one can write for the components of the electrical conductivity of a system with a dimensionality d

$$\sigma_{dc} = 0.39\nu_0 e^2 \left[\frac{n(\varepsilon_F)L^{-1/2}}{kT}\right] \exp\left[-\left(\frac{T_0}{T}\right)^{1/(d+1)}\right], \tag{21a}$$

$$\sigma_{ac} = \frac{2}{3}\pi^2 e^2 kT n^2(\varepsilon_F) L^5 \nu_e \left[\ln\frac{\nu_0}{\nu_e}\right]^4, \tag{21b}$$

where ν_0 is the limiting hopping frequency approximately equal to the frequency of the optical lattice phonon ($\nu_{ph} \sim 10^{13}$ s^{-1}).

Using the experimental values of $n(\varepsilon_F)$ and the $\sigma_{dc}(T)$ relations, it is possible to determine $\nu_0 \approx 3.2\times10^{13}$ s^{-1}. Table 4 presents the constants L, T_0, and Δ_3 for different PANI samples. It follows from the data presented that the polaron localisation length is approximately equal to the coherence length for the crystalline domains in the ES form of PANI,[71] which indicates the 3D-delocalisation of electrons in these regions.

In PANI with $z = 0.53$, charge is transferred between crystalline quasi-metallic domains with a characteristic size 6.8 nm (Table 4), located at a distance $R = 0.25L(T_0/T)^{1/2} = 4.2$ nm

($T = 300$ K). The domain consists of polymer chains rolled as a bundle in which the 3D-electron transfer predominates and intense spin–spin exchange takes place. The appearance of a Dyson-like line was recorded in the EPR spectrum of the sample as a consequence of the increase in its conductivity (Fig. 5). Assuming that the characteristic size of the particles is $r_0 \approx 2 \times 10^{-6}$ m, it is possible to calculate the alternating current electrical conductivity of the polymer at room temperature: $\sigma_{\omega c} = 2.5 \times 10^5 r_0^{-2} \nu_e^{-1} = 4.5 \times 10^5$ S m^{-1}. Next, the constants T_c and L for an individual domain ($T_0 = 2100$ K and $L = 2.5$ nm) may be determined from Eqn (21b). 3D-Hopping of the polarons takes place within the limits of the domain at a rate $\nu_{3D} = 1.6 \times 10^{12}$ s^{-1} over a distance $R = 0.39L(T_0/T)^{1/4} = 1.6$ nm at $T = 300$ K. The latter value exceeds significantly the interchain distance as a consequence of the structural disorder in the crystalline domains. The rate of the 1D-diffusion of the polaron at room temperature, determined from the line width of the 3 cm EPR spectrum, is $\nu_{1D} = 2.0 \times 10^{12}$ s^{-1}. The similarity of the rates of diffusion of the polaron along polymer chains and between the chains confirms the quasi-three-dimensional isotropic diffusion of the spin charge carrier in the oxidised polymer. The rate of charge transfer in the vicinity of the Fermi level proved to be $\nu_F = (2\Delta_2 n_e^{-1})^{1/2} = 4.6 \times 10^5$ m s^{-1}.

Thus the 2 mm EPR spectroscopic data obtained confirm the existence in PANI of highly conducting domains dispersed in the amorphous EB phase. On oxidation of the polymer, the number and size of such domains increase and there is also an increase in the dimensionality of the system. This process is accompanied by an increase in the number of Pauli charge carriers and also by an increase in the concentration of polarons. The transition from the EB to the ES form of PANI leads to an increase in the rates of relaxation and electrodynamic processes and to a change in the mechanism of charge transport in the polymer. In the oxidised sample with $z \geqslant 0.3$, the concentration of paramagnetic centres is approximately equal to the concentration of charge carriers. This permits the conclusion that there is 1D-charge transfer between the quasi-metal domains and 3D-charge transfer in the polaron lattice of these domains by polarons with a small radius in the ES form of PANI.

VI. Polytetrathiafulvalene

The 3 cm EPR spectra of powder-like polytetrathiafulvalene samples, in which the monomer TTF units are linked by phenyl (PTTF-1) or tetrahydroanthracene (PTTF-2) bridges, represents a superposition of the strongly anisotropic spectrum of immobilised paramagnetic centres with $g_{xx} = 2.0147$, $g_{yy} = 2.0067$, and $g_{zz} = 2.0028$ and the almost symmetrical spectrum of mobile polarons with $g = 2.0071$.[8,67,68] The relatively high value of the g-tensor of the radicals indicates an appreciable interaction of the unpaired electron with the sulfur atom nucleus. The spin–lattice relaxation time of the neutral PTTF-1 sample exhibits a temperature dependence of the type $\tau_1 \sim T^{-\alpha}$, where $\alpha \approx 2$ at $100 < T < 150$ K and $\alpha = 1$ at $150 < T < 300$ K.[67,68] Doping or heating of the matrix leads to the appearance of a large number of mobile paramagnetic centres and a change in their magnetic and relaxation parameters as a consequence of the conversion of the bipolarons into paramagnetic polarons. However, owing to the low spectral resolution, it proved impossible to analyse using the 3 cm EPR spectra the influence of the relaxation and dynamic parameters of the initial paramagnetic centres on the conducting properties of PTTF in greater detail.

The nature, composition, and dynamics of various paramagnetic centres in the initial and iodine-doped PTTF samples were investigated in greater detail at the 2 mm EPR band.[18,23,69]

Figs 10*a* and 10*c* present the EPR absorption spectra of PTTF, from which it is possible to determine more accurately all the components of the g-tensor and also to identify the lines attributed to different paramagnetic centres. Computer simulation demonstrated the presence in PTTF of two types of

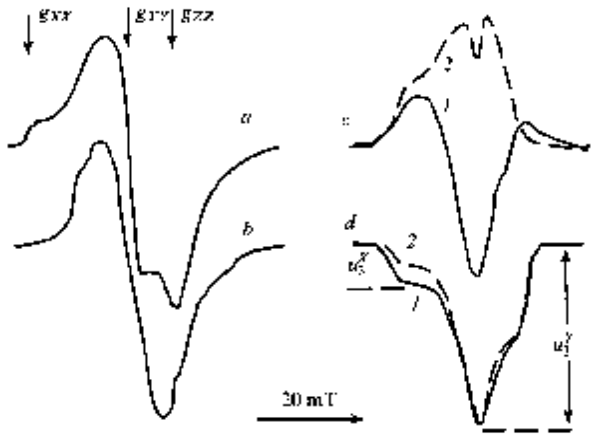

Figure 10. Typical 2 mm EPR absorption spectra (*a*, *c*) and also the spectra of the in-phase (*b*) and $\pi/2$ out-of-phase (*d*) components of the dispersion signals of the initial (*a*) and doped (*c*) polytetrathiafulvalene samples recorded at $T = 300$ K (*1*) and $T \leqslant 150$ K (*2*). The measured magnetic parameters are indicated.

paramagnetic centres with temperature-independent components of the g-tensors. The anisotropic spectrum of PTTF-1 is characterised by the magnetic parameters $g_{xx} = 2.01424$, $g_{yy} = 2.00651$, and $g_{zz} = 2.00235$, whereas the paramagnetic centres with an almost symmetrical spectrum are recorded with $g^P = 2.00706$. The principal values of the g-tensor of the paramagnetic centres localised in PTTF-2 are $g_{xx} = 2.01292$, $g_{yy} = 2.00620$, and $g_{zz} = 2.00251$, while the paramagnetic centres with a weakly asymmetric spectrum are characterised by the parameters $g_\parallel^P = 2.00961$ and $g_\perp^P = 2.00585$. The ratio of the paramagnetic centres with different forms of the spectrum is 1 : 1.8 for PTTF-1 and 3 : 1 for the neutral PTTF-2.

Since the average g-factors $\langle g \rangle$ for both types of paramagnetic centres are approximately equal, one may conclude that, as in other conducting polymers, there are in PTTF paramagnetic centres with different mobilities, namely polarons diffusing along polymer chains at a rate $\nu_{1D}^0 \geqslant 5 \times 10^9$ s^{-1} and polarons pinned on traps and/or on short polymer chains.

On doping, the comparatively large iodine ions are incorporated into the polymer matrix, increasing the mobility of its polymer chains. This is apparently the cause of the increase in the number of delocalised polarons (Fig. 10*c*). The components of the g-tensor of the mobile paramagnetic centres in PTTF-1 are fully averaged, whereas in the case of PTTF-2 such averaging takes place only partially. This finding can be accounted for by the different nature and conformations of the monomer units of the polymers.

The width of the spectral components ΔB_{PP}^{pc} of the paramagnetic centres trapped in PTTF-1 depends only slightly on temperature. However, ΔB_{PP}^{pc} for these paramagnetic centres depends on the recording frequency, increasing from 0.28 to 0.38 and then to 3.9 mT ($T \approx 270$ K) with increase in the recording frequency from 9.5 to 37 and then to 140 GHz respectively. The value ΔB_{PP}^{mob} for mobile polarons changes under these conditions from 1.0 to 1.12 and then to 17.5 mT. The fact that the mobile paramagnetic centres have a wider line than the pinned centres can be accounted for by their stronger interaction with the dopant molecules. This is typical for conducting polymers,[23,30] but conflicts with the 3 cm EPR data obtained previously for PTTF-1.[67,68]

Following a decrease in temperature by a factor of 2, the components of the spectrum of the mobile polaron in PTTF-1 are narrowed by 2.2 mT, which indicates an increase in the mobility of the polaron. Such a change in ΔB_{PP}^{mob} is analogous to the narrowing of the lines of the spin charge carriers in classical metals.

In the range of resonance frequencies $37 \leqslant \nu_e \leqslant 140$ GHz, the line width for the paramagnetic centres varies in accordance with Eqn (8), which indicates a weak interaction between the spin packets in this polymer. As a result of this, at the 2 mm EPR band the paramagnetic centres in PTTF are saturated for relatively low values of B_1, so that rapid passage effects are manifested in the in-phase and $\pi/2$ out-of-phase components of the dispersion signal (Figs 10*b* and 10*d*). Since the inequality $\omega_m \tau_2 \geqslant 1$ is valid for the neutral PTTF-2 sample, its dispersion signal U is determined mainly by the last two terms of Eqn (9). Since the condition $\omega_m \tau_1 \leqslant 1$ holds for the doped samples, their dispersion signal is determined by the u_1 and u_2 terms of this equation.

Modelling of the dispersion spectra showed that they are a superposition of the dominant asymmetric spectrum of the localised polarons with $g_{XX} = 2.01356$, $g_{YY} = 2.00603$, and $g_{ZZ} = 2.00215$ for PTTF-1 and $g_{XX} = 2.01188$, $g_{YY} = 2.00571$, and $g_{ZZ} = 2.00231$ for the neutral PTTF-2 and of the spectrum of mobile polarons (Fig. 10*b*).

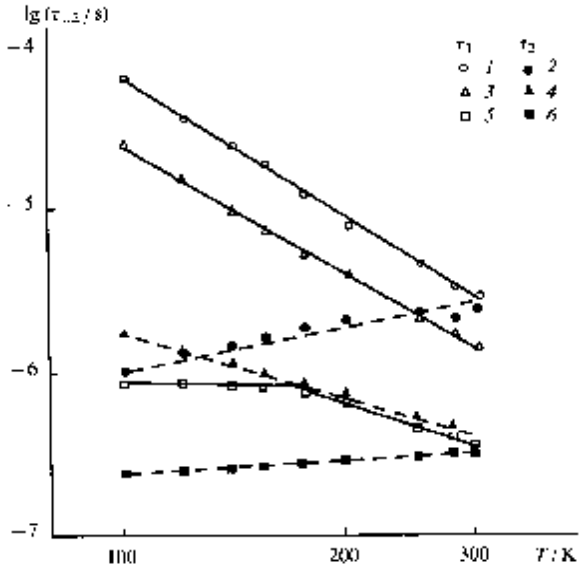

Figure 11. Temperature variations of the effective spin–lattice (τ_1) and spin–spin (τ_2) relaxation times of the paramagnetic centres in polytetrathiafulvalene-1 samples with the doping level $z = 0.4$ (*2*) and also of polytetrathiafulvalene-2 with the doping levels $z = 0$ (*1*) and 0.1 (*3*).

Fig. 11 presents the temperature variations of the effective relaxation times of the paramagnetic centres in both PTTF samples calculated from the 2 mm EPR spectra by the equations presented above. The time τ_1 varies with temperature in accordance with the $T^{-\alpha}$ law, where $\alpha \geqslant 3$ for the trapped and mobile polarons. The exponent α exceeds the corresponding value obtained previously by the spin echo method in the 3 cm EPR band.[67] The slight difference between the time τ_1^{mob} and τ_1^{loc} may be induced, for example, by the strong interaction between the different paramagnetic centres.

It is seen from Fig. 10*d* that an increase in temperature leads to an increase in the parameter $K_{mov} = u_2^Y / u_1^Y$. As in the case of PANI, this is a result of the anisotropic librational reorientations of the pinned polarons about a specified X axis of the polymer chains. The correlation time of such molecular motions, calculated by the method described by the present author,[23] was

$$\tau_c = 9.8 \times 10^{-6} \exp\left(\frac{0.02}{kT}\right) \text{ s}$$

for the PTTF-1 sample with the maximum value $\tau_c \approx 10^{-4}$ s ($T = 75$ K). The activation energies for the librations and the interchain charge transfer in the doped PTTF-1 are comparable,[67, 69] which indicates interaction of the pinned and mobile polarons in this polymer matrix.

The degree of saturation transfer depends not only on the dynamics and anisotropy of the magnetic parameters of the paramagnetic centres but also on the level of doping of the polymer. Thus the correlation time for the chain librations of the PTTF-2 samples, determined by the ST-EPR method, was

$$\tau_c = 5.2 \times 10^{-6} \exp\left(\frac{0.02}{kT}\right) \text{ s}.$$

On doping, the chains of this polymer become more rigid, which leads to a higher slope of the Arrhenius relation for this sample.[23]

$$\tau_c = 2.4 \times 10^{-6} \exp\left(\frac{0.04}{kT}\right) \text{ s}.$$

As in the case of PANI, both 1D-diffusion and 3D-hopping of the polaron at rates ν_{1D} and ν_{3D} respectively take place in PTTF. Figs 12 and 13 present the temperature variations of these rates for PTTF-1 and PTTF-2 respectively calculated by Eqns (16) and (17) using the data presented in Fig. 11. If one assumes a spin delocalisation on the polaron equal to five monomer units, then

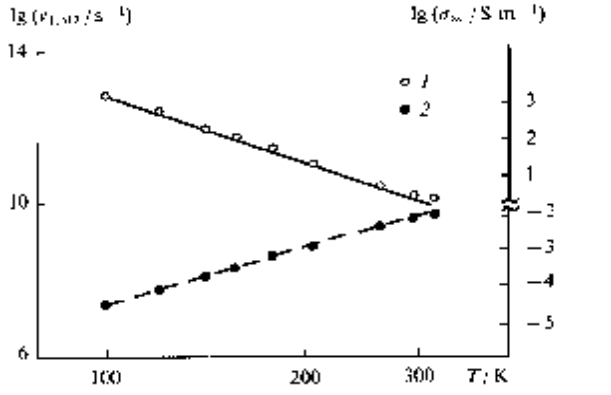

Figure 12. Temperature variations of the rates of diffusion of the polarons along the chain (ν_{1D}) and between the chains (ν_{3D}) and of the electrical conductivity σ_{ac} calculated within the framework of the isoenergetic (continuous line) and activated (dashed line) interchain charge transfer in polytetrathiafulvalene-1 with the doping level $z = 0.4$.

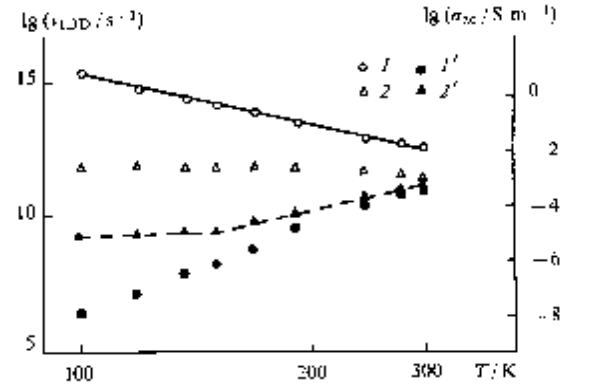

Figure 13. Temperature variations of the rates of diffusion of the polarons along the chain (ν_{1D}) and between the chains (ν_{3D}) in polytetrathiafulvalene-2 samples with the doping levels $z = 0$ (*1*, *1′*) and 0.1 (*2*, *2′*) and also of the electrical conductivity σ_{ac} calculated within the framework of the isoenergetic (continuous line) and isoenergetic-activated (dashed line) interchain charge transfer

ν_{1D} is 2×10^{10} s^{-1} for PTTF-1 and 2×10^{12} s^{-1} for the neutral PTTF-2 sample at room temperature. This quantity is smaller by at least two orders of magnitude than the frequency of the spin 1D-diffusion in PP[70] and PANI[33] obtained previously by magnetic-resonance methods at low recording frequencies, but exceeds the frequency ν^0_{1D} calculated earlier. The anisotropy of the spin dynamics ν_{1D}/ν_{3D} in PTTF at room temperature exceeds 10 and increases as the temperature is reduced.

Evidently the spin dynamics play a significant role in the charge transfer process. When the diffusion coefficients of the spins and charge carriers are equal and for $N_2 = 6.9\times10^{-3}$ of an electron per monomer unit, the components of the conductivity of PTTF-1, calculated by Eqn (4), are $\sigma_{1D}\approx0.1$ and $\sigma_{3D}\approx4\times10^{-3}$ S m^{-1} at room temperature. The value σ_{1D} obtained exceeds significantly the electrical conductivity of the sample measured using a direct current ($\sigma_{dc}\approx10^{-3}$ S m^{-1}).[67] Indeed, the macroscopic parameter σ_{dc} which reflects the hopping charge transfer between polymer chains, should not exceed the microconductivity, because $\nu_{1D}\gg\nu_{3D}$. Taking into account the different temperature variations of the conductivities σ_{1D} and σ_{3D} and also the charge transfer in PTTF by polarons with a small radius,[65] one may postulate that isoenergetic charge transfer takes place in this sample.[60]

As can be seen from Fig. 12, the function $\nu_{1D}(T)$ correlates satisfactorily with the function $\sigma_{1D}(T) = 2.4T^{-1}(81-13.6\ln T)^4$ calculated from Eqn (18b) within the framework of the approach considered. According to Eqn (18a), the isoenergetic charge transport should also lead to the temperature dependence $\sigma_{dc}(T)\approx T^{12.6}$, but the experimental σ_{3D} has a temperature variation of the type[67]

$$\sigma_{3D}(T)\sim\exp\left(-\frac{E_a}{kT}\right).$$

Thus the dynamic process considered must be analysed within the framework of thermally activated polaron hops to the edges of the conductivity band.

Indeed, the temperature variation of the rate of diffusion ν_{1D} for the PTTF-1 sample can be fitted satisfactorily by the function (20b) with $\sigma_0 = 8.3\times10^{-14}$ S s m^{-1} K^{-1}, $\nu_e = 1.4\times10^{11}$ s^{-1}, $\gamma = 0.8$, and $E_a = 0.04$ eV (Fig. 13). The value of E_a obtained is close to the activation energy for the interchain charge transfer ($E_a = 0.03$ eV) at low temperatures.[67,68] Furthermore, this quantity corresponds to the activation energy for the librations of the chains in PTTF calculated above. This fact permits the conclusion that the conductivity of PTTF is determined predominantly by the interchain phonon-assisted polaron hopping.

The probability of charge transfer is determined by the strength of the interaction of the electron with the lattice, the interchain transfer of which is accompanied by the absorption of a minimal number m of lattice phonons. It follows from Fig. 12 that the rate of the interchain spin transfer in PTTF-1 varies with temperature in accordance with the law $\nu_{3D}\approx T^{4.7}$. On the other hand, the spin–lattice relaxation time of the paramagnetic centres has a temperature dependence of the type $\tau_1(T)\approx T^{-3.6}$ (Fig. 11), which is a consequence of a multiphonon process. Adopting $E'_a = m\hbar\nu_{ph}$ and assuming that the averaged value $\langle m\rangle = 4.2$, one may calculate ν_{ph} for phonons in this sample as $\nu_{ph} = 2.5\times10^{13}$ s^{-1}, which is typical for conducting polymers. Thus, as a consequence of the strong electron–phonon interaction, the conductivity of the polymer is initiated by the librations of the polymer chains and is determined by multiphonon processes.

On passing from PTTF-1 to PTTF-2, the frequency ν_{3D} increases approximately by two orders of magnitude at room temperature (Figs 12 and 13), which is apparently associated with the more planar conformation of the monomer units in PTTF-2. Indeed, the g_{XX} parameter of the g-tensor changes by $\Delta g_{XX} = 1.32\times10^{-3}$ in this transition. Bearing in mind the dependence of the overlap integral I and the spin density on the sulfur nucleus ρ_S on the dihedral angle θ in the form $I\sim\cos\theta$ and $\rho_S\sim\sin\theta$,[13] it is possible to calculate by Eqn (1) the change $\Delta\theta$ in such a transition, which amounts to 22°. We may note that a similar conformational change occurs on passing from the benzenoid to the quinonoid form of PPP[12] and also on transition from the EB to the ES form of PANI.[29]

If it is postulated that a certain number of bipolarons (concentration N_{BP}) with a charge $2e$ are present in PTTF, an attempt may be made to interpret the spin dynamics in PTTF-2 within the framework of isoenergetic electron transport.[60] The quantities n and N_{ch} may be determined from the $\nu_{1D}(T)$ relation presented in Fig. 13: $n = 12.2$ and $N_{ch} = N_{BP} = 7.5\times10^{-5}$. Using the values $N = 2\times10^{23}$ m^{-3} and $c_{1D} = 1.2$ nm, as well as the data presented in Fig. 13, it is possible to calculate by Eqn (4) the conductivity σ_{1D}, which amounts to 1.8 S m^{-1} at room temperature. Adopting $\xi_{\parallel} = 6$ nm, $\xi_{\perp} = 0.6$ nm, $N_a = N_b = 6.7\times10^{-3}$, $N_0 = 0.11$, and $\sigma_{dc} = 2\times10^{-6}$ S m^{-1},[67] we obtain from Eqns (18) $R_0 = 4.1$ nm, $\gamma(T) = 4.0\times10^{-23}T^{13.2}$ s^{-1}, and $N_t = 3.3\times10^{24}$ m^{-3}. Fig. 13 shows that the $\sigma_{1D}(T)$ relation, derived from Eqn (18a) for a neutral PTTF-2 sample, fits the function $\nu_{1D}(T)$ fairly satisfactorily.

The rate of diffusion of the polaron in doped PTTF-2 samples varies approximately linearly in the region of low temperatures and is characterised by a high slope at higher temperatures (Fig. 13). This justifies the assumption that the charge transfer in the PTTF polymers is effected within the framework of the variable range hopping model at low temperatures with a contribution by the activated charge transfer at higher temperatures. Putting $L = \xi$, $d = 3$, and $\nu_0 = \nu_{ph} = 3.6\times10^{13}$ s^{-1}, it is possible to determine by Eqn (21) $T_0 = 7.8\times10^7$ K and $a(c_F) = 7.9\times10^{-4}$ eV^{-1} monomer^{-1} for these polymers.

The high-temperature part of the $\nu_{3D}(T)$ relation is described satisfactorily by Eqn (20b) for $\gamma = 0.8$ and $E_a = 0.035$ eV (Fig. 13). The latter quantity is close to the activation energies for the superslow librations of the PTTF polymer chains and also for the interchain charge transfer in PTTF-1. This finding indicates a close relation between the molecular dynamics and the charge transfer process in PTTF and confirms the earlier hypothesis[71] that the fluctuations of the lattice vibrations, including librations, may modulate the interchain electron transfer integral for conducting compounds. The polymer chains in PTTF-1 are less rigid than in PTTF-2, so that the above modulation in this polymer occurs at lower temperatures (Figs 12 and 13).

The intensification of the libron–exciton interactions at high temperatures indicates the formation in doped PTTF of complex quasi-particles — a molecular-lattice polaron.[72] Within the framework of this phenomenological model, it is postulated that the molecular polaron, the mobility of which is characterised by the temperature variation $\mu_m\sim T^{-1}$, is additionally coated by a lattice polarisation shell. Since the mobility of the lattice polaron μ_l is expressed by an activation function, the resultant mobility of the molecular-lattice polaron is expressed by the sum

$$\mu(T) = \mu_m(T) + \mu_l(T) = aT - b\exp\left(-\frac{E_a}{kT}\right). \qquad (22)$$

where a and b are constants. Since the formation energies of the molecular polaron in PTTF and polyacetylene crystals are similar, $E_{pm} = 0.15$ eV,[73] it is possible to determine the formation energy of the molecular-lattice polaron in PTTF as $E_{pml} = E_{pm} + E_{pl} = 0.19$ eV. The time necessary for the polarisation of the atomic and molecular orbitals of the polymer is then $\tau_e\approx\hbar E^{-1}_{pml} = 2.2\times10^{-14}$ s at room temperature. This time is significantly shorter than the characteristic polaron diffusion time in PTTF, i.e. the minimum time of the 1D- and 3D-hops of the charge carriers exceeds significantly the polarisation time of the microenvironment of these carriers in the polymer: $\tau_{1i}\gg\tau_e$. Consequently this inequality is a necessary and sufficient condition for the electronic polarisation of the polymer chains by the charge carriers.

The Fermi velocity v_F of the polarons in PTTF is 1.9×10^5 m s^{-1} (see Ref. 23) and is close to the corresponding value for PANI. The length of the free path l^* of the charge carrier in different PTTF specimen is $l^* = \nu_{1D} c_{1D} v_F^{-1} = 10^{-2} - 10^{-4}$ nm. The latter quantity is too small to regard the PTTF polymer as a quasi-one-dimensional metal.

Thus both 1D- and 3D-spin dynamics occur in PTTF, influencing significantly the charge transfer processes. The conductivity of the polymer is determined mainly by the interchain transfer of the positive charge, but, in the analysis of the transport properties of PTTF, account must also be taken of the 1D-diffusion of the spin and spin-free charge carriers.

VII. Conclusion

The data obtained demonstrate clearly the advantages of the EPR method in the study of conducting polymers at the 2 mm band. The high spectral resolution with respect to the g-factor achieved in this range makes it possible to record more accurately and separately the components of the g-tensor of organic radicals and hence makes it possible to analyse more fully and correctly the magnetic parameters of paramagnetic centres with different mobilities. The combination of a high resolving power with a low spin–spin cross-interaction permits a more effective employment of the paramagnetic centre steady-state saturation and saturation transfer methods as well as the spin label and probe method for the investigation in this frequency band of the detailed characteristics of the anisotropic molecular and spin dynamics in organic polymeric semiconductors.

The data presented demonstrate the great variety of the electronic processes occurring in organic conducting polymers. The fundamental properties of polymeric semiconductors are determined by the structure and conformation of the polymer chains, the nature and amount of the dopant introduced, and, in the first place, by the dynamics of the nonlinear excitations of the polarons and bipolarons participating in the charge transfer.

The polarons are formed on the chains of the polymer in the initial stage of its doping. With increase in the doping level, they may recombine into bipolarons. Incidentally, this process may be hindered by the structural or conformational characteristics of the polymer. The charge transfer mechanism changes on doping. Thus the conductivity of a neutral and lightly doped polymer are determined largely by the isoenergetic tunnelling of the charge between polymer chains, which is characterised by a fairly strong interaction of the spins with the lattice phonons. At an intermediate doping level, the charge is as a rule transferred by an activated mechanism and this process is initiated by the superslow anisotropic librations of the polymer chains. Finally, the variable range hopping interchain charge transfer, accompanied by comparatively weak scattering of electrons by the lattice phonons, predominates in the relatively highly conducting polymers.

References

1. H Meier *Top. Curr. Chem.* **61** 85 (1976)
2. J M Williams, J R Ferraro, R J Thorn, K D Carlson, U Geiser, H H Wang, A M Kini, M-H Whangbo *Organic Superconductors (Including Fullerenes): Synthesis, Structure, Properties, and Theory* (Englewood Cliffs, NJ: Prentice-Hall, 1992)
3. P Day, in *Handbook of Conducting Polymers* Vol. 1 (Ed. T E Scotheim) (New York: Marcel Dekker, 1986) p. 117
4. G E Wnek, in *Handbook of Conducting Polymers* Vol. 1 (Ed. T E Scotheim) (New York: Marcel Dekker, 1986) p. 205
5. T E Scotheim (Ed.) *Handbook of Conducting Polymers* Vols 1, 2 (New York: Marcel Dekker, 1986)
6. H Kuzmany, M Mehring, S Roth (Eds) *Electronic Properties of Polymers* (Berlin: Springer, 1992)
7. G Zerbi (Ed.) *Polyconjugated Materials* (Amsterdam: North-Holland, 1992)
8. R L Elsenbaumer, L W Shacklette, in *Handbook of Conducting Polymers* Vol. 1 (Ed. T E Scotheim) (New York: Marcel Dekker, 1986) p. 213
9. G Tourillon, in *Handbook of Conducting Polymers* Vol. 1 (Ed. T E Scotheim) (New York: Marcel Dekker, 1986) p. 293
10. G B Street, in *Handbook of Conducting Polymers* Vol. 1 (Ed. T E Scotheim) (New York: Marcel Dekker, 1986) p. 265
11. M E Jozefowicz, R Laversanne, H H S Javadi, A J Epstein, J P Pouget, X Tang, A G MacDiarmid *Phys. Rev. B. Condens. Matter.* **39** 12958 (1989)
12. J L Brédas, in *Handbook of Conducting Polymers* Vol. 2 (Ed. T E Scotheim) (New York: Marcel Dekker, 1986) p. 859
13. V F Traven' *Elektronnaya Struktura i Svoistva Organicheskikh Molekul* (The Electronic Structure and Properties of Organic Molecules) (Moscow: Khimiya, 1989)
14. R R Chance, D S Boudreaux, J L Brédas, R Silbey, in *Handbook of Conducting Polymers* Vol. 2 (Ed. T E Scotheim) (New York: Marcel Dekker, 1986) p. 825
15. P Bernier, in *Handbook of Conducting Polymers* Vol. 2 (Ed. T E Scotheim) (New York: Marcel Dekker, 1986) p. 1099
16. T S Zhuravleva *Usp. Khim.* **56** 128 (1987) [*Russ. Chem. Rev.* **56** 69 (1987)]
17. L D Kispert, L A Files, J E Frommer, L W Shacklette, R R Chance *J. Chem. Phys.* **78** 4858 (1983)
18. H-K Roth, V I Krinichnyi *Makromol. Chem., Makromol. Symp.* **72** 143 (1993)
19. R L Elsenbaumer, P Delannoy, G G Muller, C E Forbes, N S Murthy, H Eskhardt, R H Baughman *Synth. Met.* **11** 251 (1985)
20. O Ya Grinberg, A A Dubinskii, Ya S Lebedev *Usp. Khim.* **52** 1490 (1983) [*Russ. Chem. Rev.* **52** 850 (1983)]
21. V I Krinichnyi *Zh. Prikl. Spektrosk.* **52** 687 (1990) [*Appl. Magn. Reson.* **2** 29 (1991)]
22. V I Krinichnyi *J. Biochem. Biophys. Methods* **23** 1 (1991)
23. V I Krinichnyi *2-mm Wave Band EPR Spectroscopy of Condensed Systems* (Boca Raton, FL: CRC Press, 1995)
24. V I Krinichnyi *Usp. Khim.* **65** 84 (1996) [*Russ. Chem. Rev.* **65** 81 (1996)]
25. L M Goldenberg, A E Pelekh, V I Krinichnyi, O S Roshchupkina, A F Zueva, R P Lyubovskaya, O N Efimov *Synth. Met.* **36** 217 (1990)
26. A L Buchachenko, A M Vasserman, in *Stabil'nye Radikaly* (Stable Radicals) (Moscow: Khimiya, 1973) p. 408
27. A A Bugai *Fiz. Tverd. Tela* **4** 3027 (1962)
28. C Menardo, F Genoud, M Nechtschein, J-P Travers, P Hani, in *Electronic Properties of Conjugated Polymers* (Eds H Kuzmany, M Mehring, S Roth) (Berlin: Springer, 1987) p. 244
29. M Schärli, H Kiess, G Harbeke, W Berlinger, K W Blazey, K A Müller, in *Electronic Properties of Conjugated Polymers* (Eds H Kuzmany, M Mehring, S Roth) (Berlin: Springer, 1987) p. 277
30. V I Krinichnyi, O Ya Grinberg, I B Nazarova, L I Tkachenko, G I Kozub, M L Khidekel' *Izv. Akad. Nauk SSSR, Ser. Khim* 467 (1985)
31. V I Krinichnyi, A E Pelekh, Ya S Lebedev, L I Tkachenko, G I Kozub, A L Barra, L C Brunel, J B Robert *Appl. Magn. Reson.* **7** 459 (1994)
32. Z Wilamovski, B Oczkiewicz, P Kaiman, J Blinowski *Phys. Status Solidi B* **134** 303 (1986)
33. M Nechtschein, F Devreux, F Genoud, M Guglielmi, K Holczer *Phys. Rev. B, Condens. Matter.* **27** 61 (1983)
34. A M Vasserman, A L Kovarskii *Spinovye Metki i Zondy v Khimii i Fizike Polimerov* (Spin Labels and Probes in the Chemistry and Physics of Polymers) (Moscow: Nauka, 1986)
35. H Winter, G Sachs, E Dormann, R Cosmo, H Naarmann *Synth. Met.* **36** 353 (1990)
36. A E Pelekh, L M Goldenberg, V I Krinichnyi *Synth. Met.* **44** 205 (1991)
37. A L Buchachenko, in *Kompleksy Radikalov s Molekulyarnogo Kisloroda s Organicheskimi Molekulami* (Complexes of Radicals and Molecular Oxygen with Organic Molecules) (Moscow: Nauka, 1984) p. 158
38. A Reddoch, S Konishi *J. Chem. Phys.* **70** 2121 (1979)
39. A Abragam *Principles of Nuclear Magnetism* (London: Oxford University Press, 1961)

40. F Devreux, F Genoud, M Nechtschein, B Villeret, in *Electronic Properties of Conjugated Polymers* (Eds H Kuzmany, M Mehring, S Roth) (Berlin: Springer, 1987) p. 270
41. A A Syed, M K Dinesan *Talanta* **38** 815 (1991)
42. A J Epstein, A G MacDiarmid *J. Mol. Electron.* **4** 161 (1988)
43. M Lapkowski, E M Genies *J. Electroanal. Chem.* **279** 157 (1990)
44. A G MacDiarmid, A J Epstein, in *Science and Application of Conducting Polymers* (Eds W R Salaneck, D T Clark, E J Samuelson) (Bristol: Adam Hilger, 1991) p. 86
45. K Mizoguchi, M Nechtschein, J-P Travers, C Menardo *Phys. Rev. Lett.* **63** 66 (1989)
46. Z H Wang, E M Scherr, A G MacDiarmid, A J Epstein *Phys. Rev. B, Condens. Matter.* **45** 4190 (1992)
47. F Lux, G Hinrichsen, C Christen, V I Krinichnyi, I B Nazarova, S D Cheremisow, M-M Pohl *Synth. Met.* **53** 347 (1993)
48. S M Long, K R Cromack, A J Epstein, Y Sun, A G MacDiarmid *Synth. Met.* **55** 648 (1993)
49. J G Masters, J M Ginder, A G MacDiarmid, A J Epstein *J. Chem. Phys* **96** 4768 (1992)
50. B Z Lubentsov, O N Timofeeva, S V Saratovskikh, V I Krinichnyi, A E Pelekh, V I Dmitrenko, M L Khidekel *Synth. Met.* **47** 187 (1992)
51. A A Al'tshuller, B M Kozyrev *Elektronnyi Paramagnitnyi Rezonans Soedinenii Elementov Promezhutochnykh Grupp* (Electron Paramagnetic Resonance of Compounds of Intermediate Group Elements) (Moscow: Nauka, 1972) p. 571
52. A Carrington, A D MacLachlan *Introduction to Magnetic Resonance* (New York: Harper and Row, 1967)
53. P R Gullis *J. Magn. Reson.* **21** 397 (1976)
54. A E Pelekh, V I Kripichnyi, A Yu Brezgunov, L I Tkachenko, G I Kozub *Vysokomol. Soedin.* **33** 1731 (1991)
55. G M Burtenev, S Ya Frenkel', in *Fizika Polimerov* (The Physics of Polymers) (Leningrad: Khimiya, 1990) p. 430
56. J S Hyde, L R Dalton, in *Spin Labeling. Theory and Application* Vol. 2 (Ed. L Berliner) (New York: Academic Press, 1979) p. 1
57. M A Butler, L R Walker, Z G Soos *J. Chem. Phys.* **64** 3592 (1976)
58. K Mizoguchi, M Nechtschein, J-P Travers *Synth. Met.* **41** 113 (1991)
59. J S Blakemore *Solid State Physics* (Cambridge: Cambridge University Press, 1985)
60. S Kivelson *Phys. Rev. B, Condens. Matter.* **25** 3798 (1982)
61. A J Epstein, in *Handbook of Conducting Polymers* Vol. 2 (Ed. T E Scotheim) (New York: Marcel Dekker, 1986) p. 1041
62. G Paasch *Synth. Met.* **51** 7 (1992)
63. M El Kadiri, J P Parneix, in *Electronic Properties of Polymers and Related Compounds* (Eds H Kuzmany, M Mehring, S Roth) (Berlin: Springer, 1985) p. 183
64. P Kuivalainen, H Stubb, H Isotalo, P Yli-Lahti, C Holmström *Phys. Rev. B. Condens. Matter.* **31** 7900 (1985)
65. J Patzsch, H Gruber, in *Electronic Properties of Polymers and Related Compounds* (Eds H Kuzmany, M Mehring, S Roth) (Berlin: Springer, 1985) p. 121
66. N F Mott, E A Davis *Electronic Processes in Non-Crystalline Materials* (Oxford: Clarendon Press, 1979)
67. H-K Roth, H Gruber, E Fanghänel, Trinh vu Quang *Prog. Colloid Polym. Sci.* **78** 75 (1988)
68. H-K Roth, W Brunner, G Volkel, M Schrödner, H Gruber *Makromol. Chem., Makromol. Symp.* **34** 293 (1990)
69. V I Krinichnyi, A E Pelekh, H-K Roth, K Lüders *Appl. Magn. Reson.* **4** 345 (1993)
70. F Devreux, H Lecavelier *Phys. Rev. Lett.* **59** 2585 (1987)
71. A Madhukar, W Post *Phys. Rev. Lett.* **39** 1424 (1977)
72. E A Silin'sh, M V Kurik, V Chapek, in *Elektronnye Protsessy v Organicheskikh Molekulyarnykh Kristallakh: Yavleniya Lokalizatsii i Polyarizatsii* (Electronic Processes in Organic Molecular Crystals: Localisation and Polarisation Phenomena) (Riga: Zinatne, 1988) p. 177
73. E A Silinsh, in *Proceedings of the XIth Symposium on Molecular Crystals, Lugano, Switzerland, 1985*, p. 277